universität wien

MASTERARBEIT / MASTER'S THESIS

Titel der Masterarbeit / Title of the Master's Thesis

Light sheet microscopy of cleared mouse brains combined with immunohistochemistry.

verfasst von / submitted by

Marko Pende, BSc MSc

angestrebter akademischer Grad / in partial fulfilment of the requirements for the degree of

Master of Science (MSc)

Wien, 2015 / Vienna 215

Studienkennzahl lt. Studienblatt / degree programme code as it appears on the student record sheet:	A 066830
Studienrichtung lt. Studienblatt / degree programme as it appears on the student record sheet:	Masterstudium Molekulare Mikrobiologie und Immunbiologie
Betreut von / Supervisor:	Dipl.Phys. Univ.Prof. Dr. Hans Ulrich Dodt

Index

1. Zusammenfassung

In den letzten Jahren gab es sehr große Fortschritte in der "light sheet microscopy" und optischen Klärungsmethoden von undurchsichtigem Gewebe. Auf der einen Seite wurde das "light sheet" homogener und dünner als ein µm, was eine hohe Auflösung in der z-Achse ermöglich, und auf der anderen Seite stabilisieren neue Klärungsmethoden die Proben besser und entfernen lichtstreuende Quellen effizienter.

Zusätzlich wurden kürzlich Objektive mit großem Arbeitsabstand und einer hohen numerischen Apertur und neue Refraktionsindex-(RI)-anpassende Chemikalien, die die Transparenz des Gewebes und das Verhältnis zwischen Signal und Hintergrund für mehrere Monate konservieren, entwickelt. Dies ermöglicht schnelle 3D-Rekonstruktion von großen Proben mit einer sehr hohen Auflösung und weniger Verlust von transgenen Signalen.

Mit der Entwicklung der zuvor erwähnten Innovationen rückte das Gebiet der Immunohistochemischen (IHC) Protokole für große Gewebe und das Visualisieren von mit Antikörpern gefärbten Strukturen in diesen Geweben in den Fokus des Interesses.

In dieser Arbeit evaluiere ich verschiedene optische Klärungsmethoden in der Kombination mit diversen Protokollen für Immunfärbung und enthülle dabei die Notwendigkeit für weitere Verbesserung, was die Inkubationszeit und die Färbegradienten der Antikörper angeht.

Weiterst habe ich die Klärungsmethode namens CLRITY optimiert, indem ich, das Entfernen von lichtstreuenden Molekülen verbessert und ein neues RI-angleichendes Mittel namens BrainClear verwendet habe. Dabei habe ich die Bearbeitungszeit der Proben um die Hälfte reduziert und den Erhalt des Grünen Fluoreszenz Proteins (GFP)-Signals gesteigert.

2. Abstract

In recent years light-sheet microscopy and tissue clearing techniques evolved quite rapidly. On one hand the light sheets became more homogeneous and thinner than one µm, which allows high resolution in the z-axis. On the other hand new clearing techniques stabilize the specimens and remove light scattering sources more efficiently.

In addition lately developed objectives with long working distances and high numerical apertures (NA) and new refraction index (RI) matching chemicals, that preserve the transparency of the tissue and the signal to background ratio for many months, enable fast 3D reconstruction of large specimens with high resolution and less transgenic signal loss.

With the development of the afore mentioned innovations, immunohistochemical (IHC) protocols for large specimens and the visualization of antibody labeled structures within thick intact tissues in three dimensions became an area of focus.

Here I evaluated diverse available clearing techniques in combination with different immunolabeling protocols and thereby showing the necessity of further improvement regarding incubation time and labeling gradients of the antibodies.

Further, I improved the clearing technique termed CLARITY by optimizing the removal of light scattering molecules and by using anew RI matching agent called BrainClear. Thereby the sample processing time was reduced by half and we were able to enhance the preservation of the green fluorescent protein (GFP)- signal.

3. Introduction

3.1 Different approaches to image thick tissue

Since decades scientist were very successful in obtaining biological information from thin tissue sections, but this 2- dimensional approach is very limited when high-resolution data from complex systems, such as individual neurons, which extend in many directions, or the vasculature, are needed. This restriction led to the development of different volumetric tissue analyzing methods, that helped to keep a global perspective required to understand such system function.

Non invasive approaches like magnetic resonance (MR) microscopy, X-ray computer tomography (CT) or optical projection tomography (OPT) could image very large specimens and provide useful insight in the development, perturbation and pathologies of humans and model organisms (Johnson et al., 2002; Kalender, 2005; Sharpe et al., 2002; Tyszka et al., 2005) but were restricted to the macroscopic scale with isotopic resolution of 20-25 µm at best.

On a microscopic scale, confocal and 2-photon microscopy have single cell resolution but could not, due to intrinsic light scattering effects of non transparent tissues, image specimens thicker than a few 100 µm (Helmchen and Denk, 2005). Therefore, high resolution imaging methods were used in combination with milling machines to obtain deeper three dimensional information from biological structures (Ragan et al., 2012; Ragan et al., 2007; Streicher et al., 2000; Weninger and Mohun, 2002).

However, this approach is technically very challenging, due the massive mechanical sectioning and the loss or deformation of individual sections during the process, that can lead to insufficient volumetric reconstruction of the gained data. Despite the mentioned obstacles, these deep imaging strategy evolved, i.e. array tomography, micro optical sectioning tomography (MOST), knife edge scanning microscopy (KESM) and optical projection tomography (OPT) and under sufficient control serial sectioning, can give rise to

very impressive results (Gong et al., 2013; Li et al., 2010; Mayerich et al., 2008; Micheva and Smith, 2007; Oh et al., 2014; Xiong et al., 2014; Zheng et al., 2013).

Another imaging possibility that eliminates the loss and alignment issues of sections are the so called block-face methods (Denk and Horstmann, 2004; Ichimura et al., 2015; Toga et al., 1997; Tsai et al., 2009). Thereby the surface of a block of tissue is imaged and sequentially shaved off to reveal the next layer surface. A major drawback in this concept is, that although it is possible to achieve sub-micrometer resolution, the sectioning obliterates the imaged tissue what makes subsequent analysis impossible.

All of these aforementioned techniques are not easy to implement and are far from standard in laboratories. After extensive use of transparent model organisms and the revival of chemical tissue clearing methods a modernized old approach (Siedentopf and Zsigmondy, 1902) became increasingly popular to study biological systems: Light sheet fluorescent microscopy (LSFM) (Figure 1).

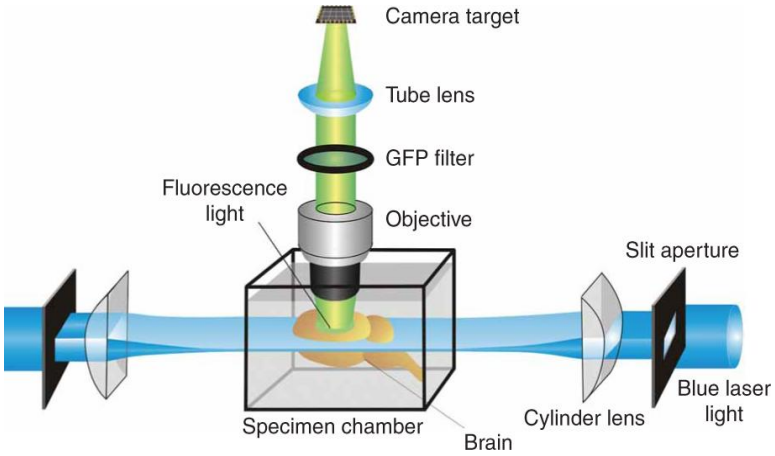

Figure 1*drawing of the optics of an ultramicroscope. Taken from (Dodt et al., 2007)*

Light sheet fluorescent microscopy, also called Ultramicroscopy or selective plane illumination microscopy (SPIM), enables the possibility of multiple imaging of large specimens without the need of mechanical sectioning and in doing so, avoiding the challenging alignment issues (Dodt et al., 2007; Huisken et al., 2004).

This approach allows, in contrast to confocal- and 2-photon microscopy, fast recording on a cellular level of optically sectioned images in chemically cleared "transparent" samples. Putting the recording speed in numbers, laser scanning techniques would need for a volume

of 1000mm^3 (approximately the size of a mouse brain), using a 20x / NA 1.0 objective, a assumed 500x500µm field of view and 1µm axial step size, more than 4.200.00 images. At a relatively fast scan rate of 1 Hz, this would take nearly 50 days (Richardson and Lichtman, 2015). In comparison, most of the LSFM concepts illuminate a whole plane and an image of the plane can be captured by a camera in a single exposure. When combined with a scientific complementary metal-oxide semiconductor (sCMOS) camera the only limiting recording factor would be the time it takes to move the sample to the next focal plane (Richardson and Lichtman, 2015).

The initial restrictive factor of these method was, that the transparency of the specimens was achieved by matching the average refractive index (RI) of the sample in a liquid medium. This required long working distance immersion objectives for imaging. Meanwhile this obstacle was overcome by commercially available, RI adjustable, large field of view immersion objectives or by RI corrected air objectives in an dipping cap (DE102013012182 A1) (Figure 2). Additionally, new super thin light sheets improved the z-resolution of the 3D reconstructed samples tremendously (Bouchard et al., 2015; Chen et al., 2014; Holekamp et al., 2008; Planchon et al., 2011; Saghafi et al., 2014; Wu et al., 2013).

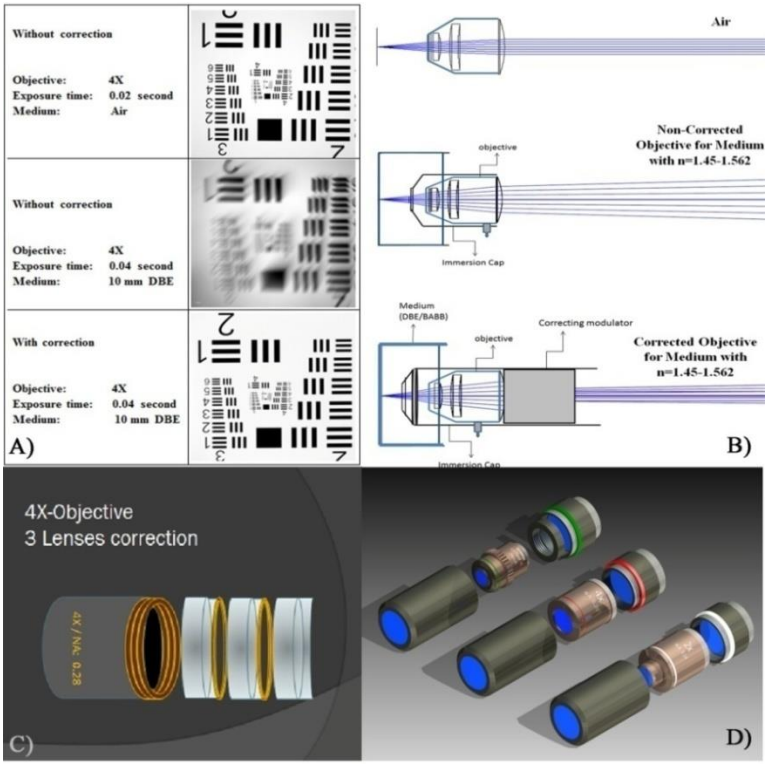

Figure 2*A) Images obtained with 4X-objective (N.A. 0.28) in air and DBE without and with correction, B) Optical arrangement for objective (without and with correction optics), C) 4X objective with correction optics, D) Three corrected air objectives , 2X (N.A. 0.14), 4X (N.A. 0.28) and 20X (N.A. 0.45). Picture and legend are taken Dodt et al., 2015.*

A big challenge, in relation to microscopy of large samples, is the opacity of most biological specimens caused by light scattering.
Scattering is due to the mismatches in the RI at the borders of biological structures i.e. membranes, organelles and cells in tissue which cause light rays to deviate many times.

The methods that aim to achieve tissue transparency have different strategies to assure a highly uniform RI, so that lateral scattering is minimized and that all wavelengths of light pass through the tissue. An additional goal is to preserve transgenic signals in the cleared tissue and to facilitate molecular labeling with i.e. immunohistochemical approaches.

3.2 Optical tissue clearing techniques

Since Spalteholz described at the beginning of the 20th century a clearing technique for large tissues using organic solvents (Spalteholz, 1914) many other methods appeared which focused on equilibrating the RI throughout the whole samples. However, the field was split into two approaches: the tissue dehydration and solvent-based and the recently emerged aqueous based clearing.

3.2.1Dehydration and solvent based clearing

Solvent-based clearing techniques consists of a dehydration step with lipid solvation and a RI-matching step with further lipid removal (Figure 3).

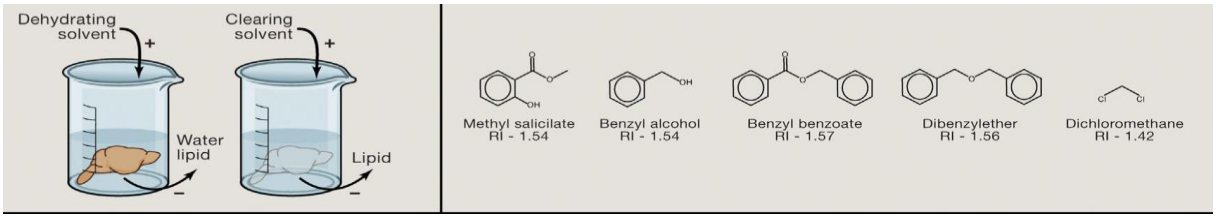

Figure 3*(Left) Solvent-based clearing is a two-step process. First, the tissue is dehydrated and lipid are removed. Second, the tissue is transferred to a high refractive index solvent where additional lipid solvation and clearing occurs. (Right) Molecules commonly used for solvent-based clearing along with the refractive indices (RI) of the pure chemical. Picture and legend are taken and adapted from Richardson and Lichtman, 2015*

Different solvents have been tested for use in either the dehydration or the clearing step (Becker et al., 2012). The tissue dehydration is now performed with tetrahydrofurane (THF) which has better fluorescence preserving properties than the former used ethanol (Becker et al., 2012; Dodt et al., 2007; Erturk et al., 2012; Spalteholz, 1914).The water and lipid removal results in a shrinked, very dense sample which mainly consists of proteins and remaining lipids (Becker et al., 2012). Because dehydrated protein has a very high RI the lipid solvable agent, that should facilitate homogeneity throughout the sample, must have a RI, greater than 1.5 .To date, methylsalicilate, benzyl alcohol-benzyl benzoate (BABB), dichloromethane and dibenzyl ether (DBE) (Figure 4) have been used as final clearing agents (Becker et al., 2012; Dodt et al., 2007; Erturk et al., 2012; Renier et al., 2014; Spalteholz, 1914; Steinke and Wolff, 2001).

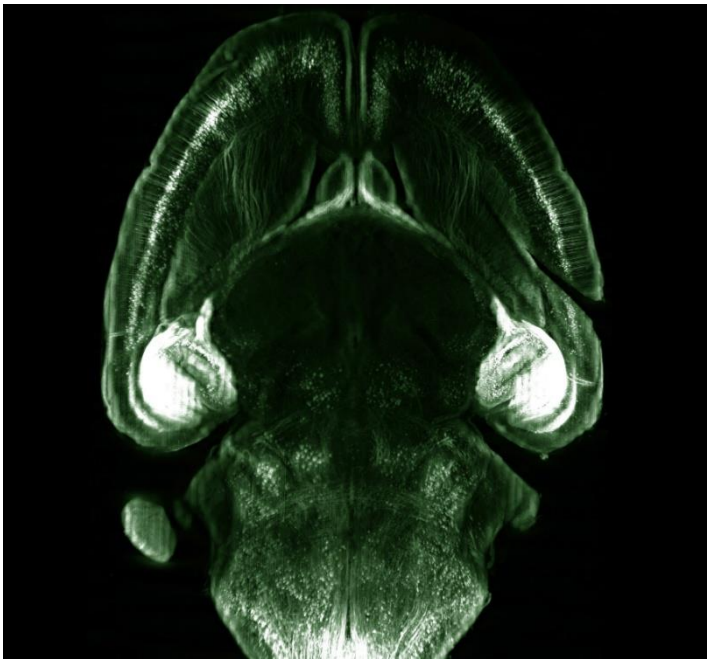

Figure 4 *Example of a tetrahydrofurane(THF) dehydrated and dibenzyl ether (DBE) cleared whole TH1-GFP-M mouse brain. Image was taken with an Ultramicroscope. Objective 1.3x / NA 0.14.Kindly provided from Christian Hahn (unpublished).*

The challenge of this approach is, that the dehydration removes water molecules from the specimens, which are necessary to maintain signal from most of the fluorescent proteins. The first attempt to address this issue was done with the methods 3DISCO (Erturk et al., 2012) and iDISCO (Renier et al., 2014). With this approaches, it was possible to maintain the

fluorescent signals for a few days. The solvent based clearing methods are easy to handle and work on a number of different tissue types, but still fluorescent protein (FP) emission reduction is a big obstacle. A possible solution to the quenching problem could be the minimization of, GFP damaging, organic peroxides in the dehydration and clearing agents (Alnuami et al., 2008).

Table 1 *Comparison of dehydration and solvent based clearing methods*

Solvent based	**Final refractive index (RI)**	**Key components**	**Time to clear**	**Alterations in tissue morphology**	**FP emission**	**Detergent used**	**Lipid preserved**
Spalteholz	1.55	Benzylbenzoate/ Methylsalicilate	Months	Shrinkage	No	No	No
BABB	1.55	Benzylbenzoate/ Methylsalicilate	Days	Shrinkage	Half day	No	No
3DISCO	1.56	Dichloromethane /Dibenzylether	Hours	Shrinkage	Yes, but only 1-2 days	No	No
iDISCO	1.56	Dichloromethane /Dibenzylether	Hours	Shrinkage	Yes, but only 2-4 days	Optionl: Triton, NP 40, Tween 20, deoxycolate	No

3.2.2 Aqueous base clearing techniques

The fluorescent signal loss and the tissue deformation, induced by dehydration caused shrinkage of the specimens, initiated the development of aqueous based clearing solutions. These techniques can be divided in three approaches: First, the tissue is immersed in a solution that is RI matched to it. Second, lipid removal followed by hydration to change the average RI. Third, passive or active lipid removal followed by immersion in a RI matching liquid.

3.2.2.1 Simple immersion approaches

Since in simple immersion techniques, lipids are not removed a RI greater than 1.45 needs to be achieved to clear a sample sufficiently.

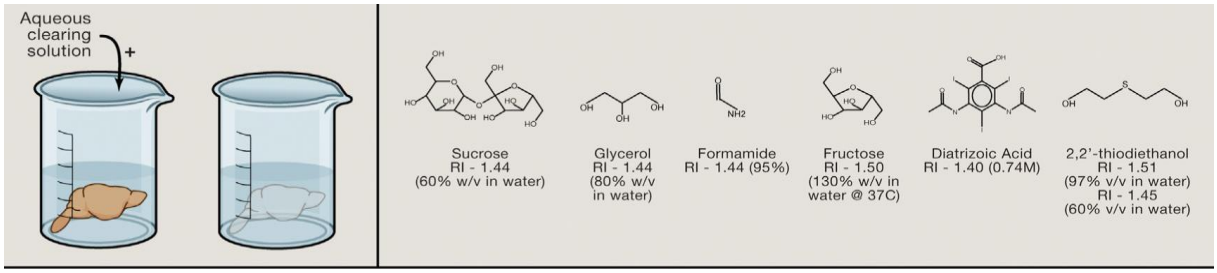

Figure5*(Left) For simple immersion, the tissue to be cleared is placed in an aqueous clearing solution for days to months. During this time, the solution is exchanged repeatedly. (Right) Molecules commonly used for simple immersion along with the refractive indices (RI) at the commonly used concentration. Picture and legend are taken and adapted from Richardson and Lichtman, 2015*

As depicted in figure 5, sucrose (Tsai et al., 2009), glycerol (Meglinski et al., 2004), foramide (Kuwajima et al., 2013), fructose (Costantini et al., 2015; Ke et al., 2013)and 2,2'-thiodiethanol (TDE) (Hou et al., 2015; Staudt et al., 2007) have all been used for this purpose. The above mentioned liquids are difficult to handle, because of the high concentration and viscosity of these mixtures, which make them susceptible for precipitation and introduced air bubbles. However, there are also simple immersion clearing solutions with lower viscosities and high RI i.e. FocusClear™ (Chiang et al., 2002) and Histodenz™ (Yang et al., 2014). In both cases the high cost and the inability of long term sample storage may limit their use. Two low cost options are TDE and the FRUIT technique. TDE is a low viscosity liquid and its RI can be adjusted by simple dilution with water (Costantini et al., 2015). One drawback of TDE is the strong reduction of the transgenic fluorescence signal, at concentrations which are sufficient for tissue clearing. FRUIT (Hou et al., 2015) is a combination of two methods, Scale (Hama et al., 2011) and SeeDB (Ke et al., 2013) , that uses a mixture of fructose with urea, resulting in low viscosity of the solution and improved tissue clearing over the two techniques used alone.

Passive clearing by immersion in high RI solutions does not clear as good as the solvent-based methods or the later discussed other aqueous-based but they are easy to implement, economical and give good results for smaller samples (Figure 6).

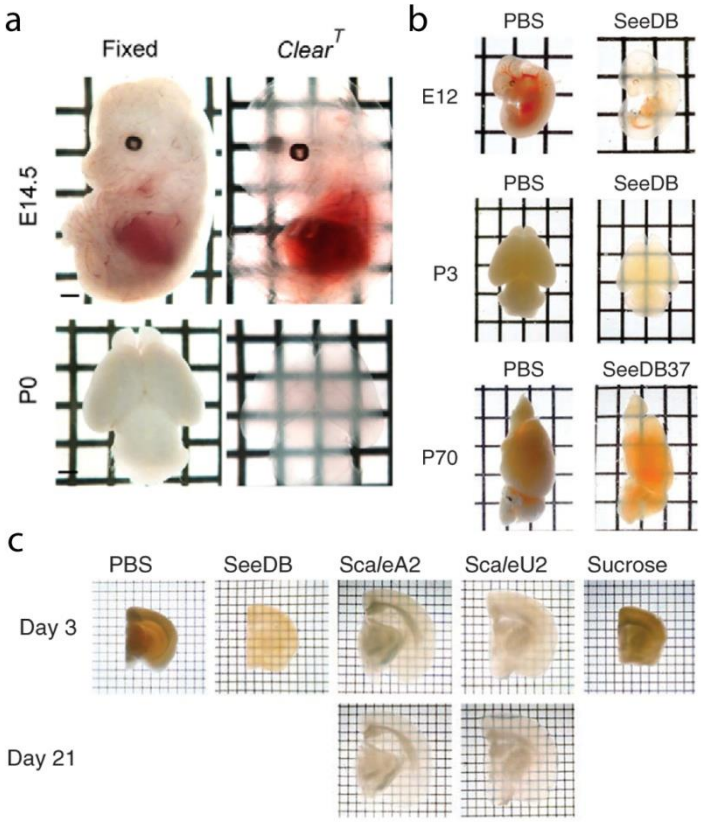

Figure 6 *Example pictures of different simple immersion approaches;(**a**) Fixed whole embryos(E14.5) and dissected postnatal brains (P0) cleared overnight with ClearT. (**b**) Whole embryos (E12), Neonatal (P3) whole-brain sample and adult hemi-brain samples (P70) were cleared with SeeDB (**c**) Adult brain slices (P66, 1.5 mm thick) cleared with various clearing agents. Grids are 1x1mm (a-b) and 2.6x3.2mm (c). Picture and legend are taken and adapted from Ke et al., 2013and Kuwajimaat al., 2013.*

Table 2 *Comparison of simple immersion based clearing methods*

Simple immersion	Final refractive index (RI)	Key components	Time to clear	Alterations in tissue morphology	FP emission	Detergent used	Lipid preserved
Sucrose	1.44	Sucrose	1 day	Shrinkage	Yes	Triton (2%)	No
FocusClear	1.47	Diatrizoic acid	Hour-Days	No	Yes	Tween 20	Yes
ClearT*	1.44	Formamide	Hour-Days	No	No	No	Yes
ClearT2*	1.44	Formamide/ PEG	Hour-Days	No	Yes	No	Yes
SeeDB	1.48	Fructose/Thioglycerol	Days	No	Yes	No	Yes
FRUIT*	1.48	Fructose/ Thioglycerol/ Urea	Days	Minimal expansion	Yes	No	Yes
TDE^	1.42	2,2'-thiodiethanol	Days-Weeks	No	Yes	Optional: 8% SDS	No

*Denotes techniques that also have a hyperhydration component
^Can be combined with CLARTIY/PACT/PARS

3.2.2.2 Hyperhydration approaches

The idea of hyperhydration techniques is to remove the lipids without hydrophobic solvents (in order to maintain an aqueous environment for fluorescent proteins)during the clearing process and to reduce thereby the average RI of the tissue (Figure 7).

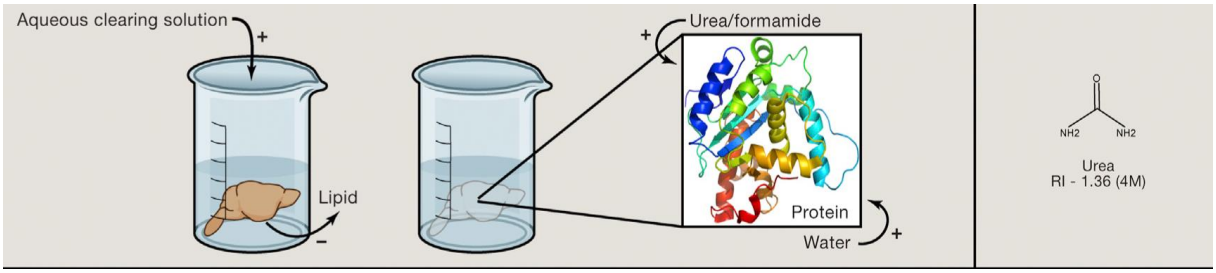

Figure 7 *Hyperhydration involves submerging the sample in an aqueous solution and allowing it to passively clear. During this clearing step, urea or formamide in the clearing solution can enter tightly folded regions of high refractive index proteins, creating an osmotic gradient that pulls in water as well. This partially denatures the protein, hydrates it, and decreases its overall refractive index. Some hyperhydration methods contain detergent that is used to disrupt membranes and remove lipid from the sample. Picture and legend are taken and adapted from Richardson and Lichtman, 2015*

Scale was the first technique that was published with this approach (Hama et al., 2011). The method use a detergent based lipid removal with a simultaneous urea mediated hydration, in the presence of glycerol, to achieve sample transparency (Figure 8 c-d). The mayor disadvantage for the Scale approach is the long incubation time (up to months) and the very swollen and fragile tissue, which results from the hyperhydration.

Another urea based method called CUBIC (Figure 8 a, b) that makes use of the hyperhydration mechanism with an optional second high-RI sucrose-based clearing step to maximize the transparency (Susaki et al., 2014; Tainaka et al., 2014). The fluorophore emission is in both cases well preserved, but CUBIC is in comparison to Scale a magnitude faster and the resulting sample is more stable, although the used high Triton X 100 levels (50%) can result in an elevated degree of protein loss.

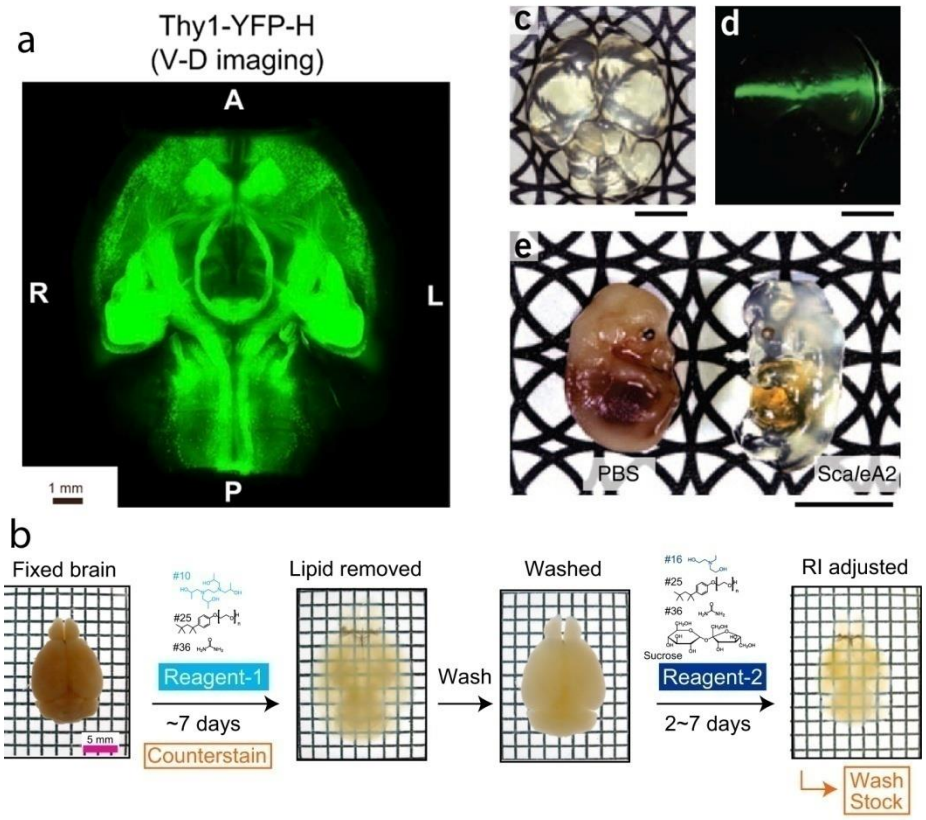

Figure 8 *Example pictures of different hyperhydration approaches; (**a**) Image of a CUBIC cleared TH1-YFP-H Tg mouse brain (2 months old) (**b**) CUBIC protocol. A fixed whole brain (from a 6-month-old mouse) was treated with reagent 1 to remove lipid components for up to 7 days, followed by washing with PBS. The sample was then treated with reagent 2 for 2–7 days to adjust the refractive indices of the tissue and reagent. (**c,d,e**) Images of Scale cleared samples. (**c,d**) A whole fixed and cleared brain of a mouse(P15) after treatment with ScaleA2 for 2 weeks. (d) The green light from a 1-mW, 532-nmlaser beam pointer traversed the cleared brain. (**e**) A photo of two embryos (E13.5). Left, embryo placed in PBS after fixation with 4% PFA. Right, embryo incubated in ScaleA2 solution for 2 weeks after fixation with 4% PFA. Picture and legend are taken and adapted from Susaki et al., 2014 and Hama et al., 2011.*

Table 3 *Comparison of hyperyhdration based clearing methods*

Hyperhydration	Final refractive index (RI)	Key components	Time to clear	Alterations in tissue morphology	FP emission	Detergent used	Lipid preserved
Scale 2A	1.38	4M Urea 10% Glycerol	Weeks	Expansion	Yes	Triton X100 (0.1%)	No
Scale 2U	1.38	4M Urea 30% Glycerol	Months	No	Yes	Triton X100	No
CUBIC	CUBIC-1 1.38 CUBIC-2 1.48	4M Urea/ 50% Sucrose	Days	Expansion	Yes	Triton X100 (50%)	No
Whole-Body CUBIC	1.38	4M Urea	Days	Expansion	Yes	Triton X100 (10%)	No

3.2.2.3 Hydrogel embedding approaches

All the techniques mentioned above induce strong tissue deformation, their clearing capacity is limited to small samples or lead to a significant protein loss due to the used high concentrations of applied detergents. The CLARITY methods attempt to address these problems by first embedding the sample in a hydrogel-polymer solution (Chung et al., 2013; Tomer et al., 2014). After this, lipids are removed actively through an electric field in an 8% sodium dodecyl sulfate (SDS) detergent solution. A final incubation in an aqueous clearing solution i.e FocusClear, Histodenz, TDE or 80% Glycerol, generate samples with very good transparency and preserved transgenic signal (Figure 10).

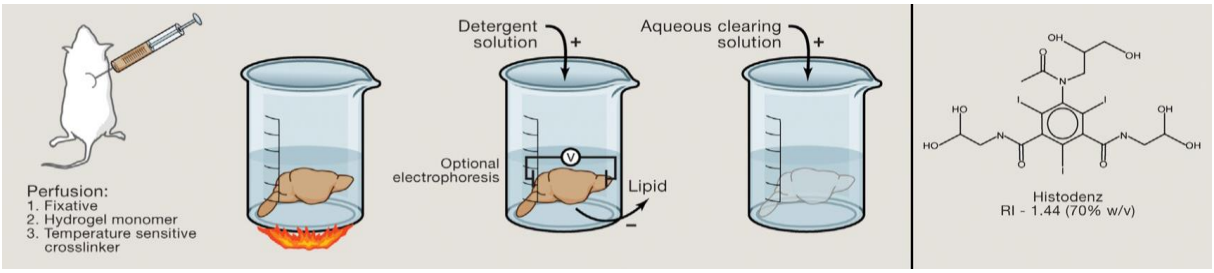

Figure 10 *(Left) Hydrogel embedding is most often performed on an entire animal by perfusing with a fixative, a temperature-sensitive crosslinker, and the hydrogel monomer. Alternatively, these chemicals can be passively diffused into an isolated tissue sample. Once fixed, the tissue of interest is warmed to induce hydrogel crosslinking. The sample is then placed in a detergent solution to remove lipid material passively or via an electrophoretic charge. Finally, the lipid-free sample is placed in a high refractive index matching solution for clearing. Histodenz is one high refractive index molecule that can be a component of this clearing solution. Glycerol, TDE, or diatrizoic acid also can play this role. Picture and legend are taken and adapted from Richardson and Lichtman, 2015.*

However, the method is very difficult to implement and tissue damage caused by the electric field led to the development of a approach called PACT/PARS (Yang et al., 2014). This approach removed the electric field from the protocol and replaced it with simple incubation in the SDS solution, which made the method very robust but also very long lasting (weeks). A recent application to hydrogel embedded tissue termed Expanse Microscopy (ExM) first labels the tissue with specific molecules, then digest the specimen with digestive enzymes and finally uses the hydrophilic properties of the polymer network to extend the sample size by a factor of 4.5. The labeled remaining hydrogel can be used to perform scalable super resolution microscopy with diffraction limited microscopes (Chen et al., 2015) (Figure 12).

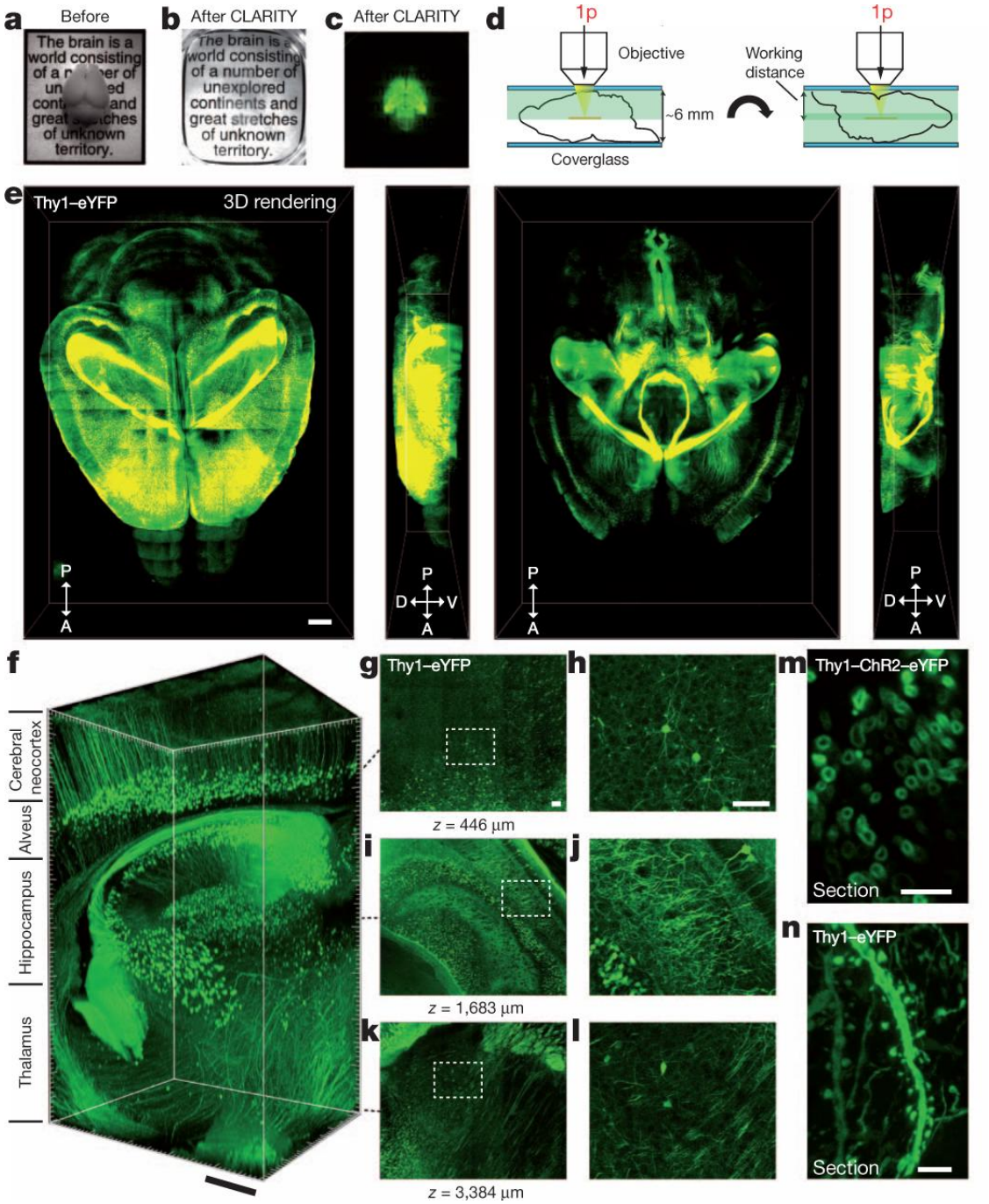

Figure 11 *Imaging was performed in adult mouse brains (3 months old). (**a**) Cajalquote before CLARITY. (**b**) Cajalquote after CLARITY: Thy1–eYFP line-H mouse brain after hydrogel–tissuehybridization, electrophoretic tissue clearing (ETC) and refractive-index matching. (**c**) Fluorescence image of brain depicted in (**b, d**) Dorsal aspect is imaged (single-photon (1p)microscopy), then brain is inverted and ventral aspect imaged. (**e**) Three dimensional rendering of clarified brain imaged (310 water-immersion objective; numerical aperture, 0.3; working distance, 3.6mm). Left, dorsal half (stack size, 3,100 mm; step size, 20 mm). Right, ventral half (stack size,3,400 mm; step size, 20 mm). Scale bar, 1mm.(**f**) Non-sectioned mouse brain tissue showing cortex, hippocampus and thalamus (310 objective; stack size, 3,400 mm; step size, 2 mm). Scale bar,400 mm. (**g–l**) Optical sections from f showing negligible resolution loss even at ,3,400-mm deep.(**h, j, l**) boxed regions in(**g, i, k**) respectively. Scale bars, 100 mm.(**m**) Cross-section of axons in clarifiedThy1–channelrhodopsin2 (ChR2)–eYFP striatum: membrane-localizedChR2–eYFP (1-mm-thick coronal block; 363 glycerol-immersion objective; numerical aperture, 1.3; working distance, 280 µm). Scale bar, 5 mm.(**n**) Dendrites and spines of neurons in clarified Thy1–eYFP line-H cortex(1-mm-thick coronal block; 363 glycerol objective). Scale bar, 5 mm. Picture and legend are taken and adapted from Chung et al., 2013.*

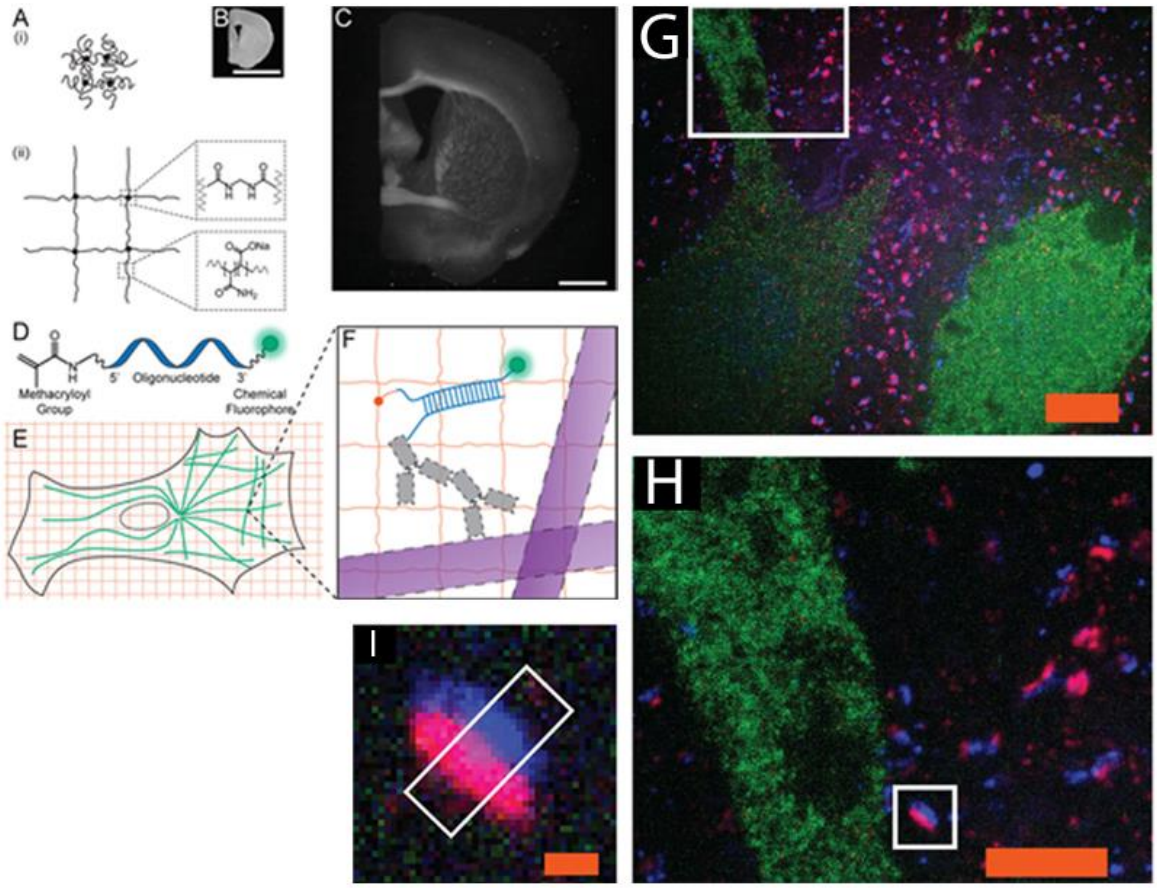

Figure 12*(**A-F**) Expansion microscopy (ExM) concept.(**A**) Scheme of a collapsed polyelectrolyte network (i), showing crosslinker (dot) and polymer chain (line), and expanded network (ii) after H2O dialysis. (**B**) Photograph of a fixed mouse brain slice. (**C**) Photograph, post-ExM, of the sample (**B**) under side illumination. (**D**) Schematic of label that can be anchored to the gel at site of a biomolecule. (**E**) Schematic of microtubules (green) and polymer network (orange). (**F**) The label of (**D**), hybridized to the oligo-bearing secondary antibody (gray) bound via the primary (gray) to microtubules (purple), is incorporated into the gel (orange lines) via the methacryloyl group (orange dot). (**G**) Confocal fluorescence images stained with pre-synaptic (anti-Bassoon, blue) and post-synaptic (anti-Homer1, red) markers, in addition to anti-GFP (green), post-(**G**) expansion. (**H**) Details of boxed regions in (**G**). (**I**) Single representative. Picture and legend are taken and adapted from Chen et al., 2015.*

Table 4 *Comparison of hydrogel embedding based clearing methods*

Hydrogel Embedding	Final refractive index (RI)	Key components	Time to clear	Alterations in tissue morphology	FP emission	Detergent used	Lipid preserved
CLARITY	1.45	FocusClear/ 80% Glycerol	Days	Slight Expansion	Yes	SDS (8%)	No
PACT	1.38-1.48	Histodenz	Days-Weeks	Slight Expansion	Yes	SDS (8%)	No
PARS	1.38-1.48	Histodenz	Days	No	Yes	SDS (8%)	No

3.3 Immunolabeling

Despite the different approaches of tissue clearing all methods which are compatible with immunolabeling protocols have one thing in common: very long antibody incubation times (weeks-months) prior to the final RI matching step. The simple reason for this is that the diffusion and binding is hindered by these highly viscous solutions. Some attempts have been made to speed up the process of immunolabeling.

To facilitate a better penetration of the antibodies, the pore size of hydrogel embedded tissue was enlarged by the reduction of the polymers in the solution. It is believed, that this lead to faster and complete immunolabeling (Yang et al., 2014) but other claim that the pore size has a negligible effect (Li et al., 2015).Another technique specially designed to perform antibody labeling called iDISCO, ether dehydrate and rehydratethe specimens or use detergents to remove all membranes to enable a better staining outcome(Renier et al., 2014). Although the results shown were impressive the transgenic signals suffers from this approach and the long antibody labeling time remains.

A more basic approach is to minimize the size and to increase the specificity of the antibodies. Thereby smaller antibodies or antibody parts i.e. from shark or camel, F(ab)2 or F(ab) parts of the antibodies, single domain antibodies, nanobodies (Holliger and Hudson, 2005)or nucleic acid aptamers (Bunka and Stockley, 2006) which are a fraction of the size of standard antibodies can better reach epitopes deep in the specimens in a shorter period of time.

Further the conjugation of fluorophore to these samples make a secondary antibody incubation step obsolete.

It was also shown that epitop retrieval and antibody binding is better and faster when incubated in special microwave PELCO BioWave® Pro or even in normal commercial microwaves under low wattage and controlled temperature (Ferris et al., 2009; Munoz et al., 2004; Owens et al., 2013; Temel et al., 2006).

Finally, a new approach facilitating a electrophoretically driven antibody delivery into cleared tissue sections (Li et al., 2015) could be utilized in principle for bigger tissue. By adapting this method larger specimens, like an entire mouse brain, they could probably be stained in a short amount of time.

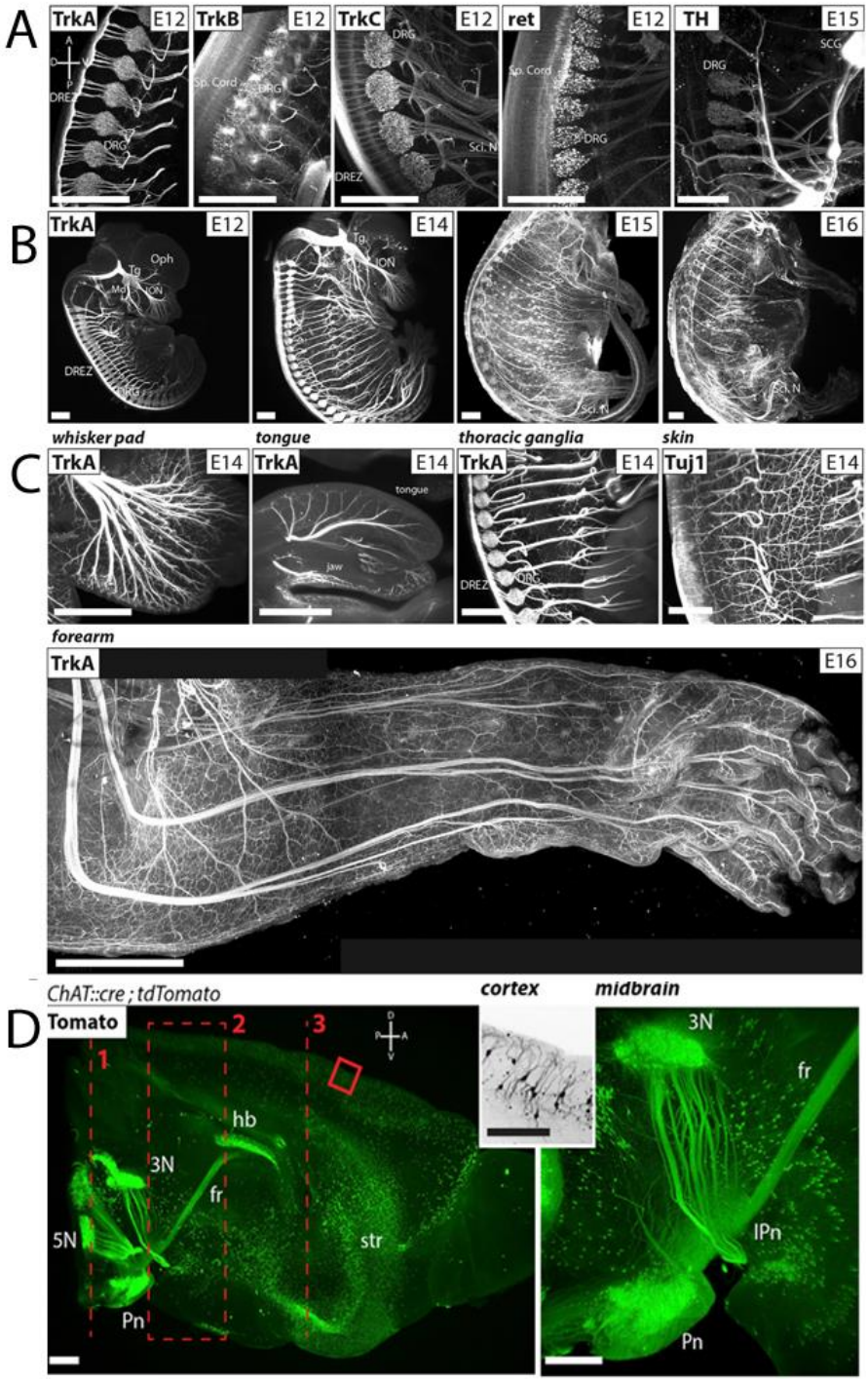

Figure 13 *iDISCO labeled specimens. (**A**) Whole-Mount Imaging of the Embryonic Peripheral Sensory Nervous System E12.5 embryos labeled for TrkA, TrkB, TrkC, and ret, and E15 embryo labeled for tyrosine hydroxylase. (**B**) Sagittal maximum projections at the level of the horacic (TrkA and TrkB), lumbar (TrkC), or cervical (ret and TH) DRGs. Half projections of whole embryos labeled for TrkA. (**C**) Details of the TrkA innervation at E14.5 in the whisker pad, tongue, and thoracic DRGs, and Tuj1-labeled innervation in the flank skin. E16.5 forearm labeled with TrkA and imaged with a two-photon microscope. (**D**) Projection of a whole-mount RFP immunolabeling of a 1-month-old mouse half forebrain from a ChAT::cre ; Rosa26lsl-tdTomato reporter line, showing details of the midbrain, cortex and optical sections at different levels. Scale bars represent 500 mm. Picture and legend are taken and adapted from Renier et al., 2014.*

3.4 Goal of work

As described above there are many approaches to achieve tissue transparency. My intention was to establish and to optimize the CLARITY method for whole mouse brain in our laboratory.

After achieving this, I wanted to perform immunohistochemical staining with CLARITY and compare this technique with other molecular labeling protocols of different clearing methods as iDISCO.

In addition, I generated Alexa-Fluorophore conjugated F(ab')2 parts to facilitate: Deeper tissue penetration by using small antibody fragments and shorter processing time by linking the fluorochrome to the primary antibody, making the incubation step with the secondary antibody redundant.

Finally, I tried to enhance the binding speed of the antibodies by using a commercial microwave.

4. Materials and Methods

4.1 Animals

Wild-type Lewis rats and TH1-GFP-M mice (Feng et al., 2000) were bred in the decentralized facilities of the Institute for Biomedical Research (Medical University Vienna) and were sacrificed at the age of six to eight weeks. They were housed under standardized pathogen-free conditions in a twelve hour night and day cycle.

Every procedure involving animals was performed in consideration of the institutional and national guidelines. The animals had free access to food and water.

4.1.1 Experimental autoimmune encephalomyelitis (EAE)

All EAEs injections were performed by Bleranda Zeka, MSc from our cooperation partner, the Lassmann Laboratory.

EAE is an animal model and can be induced by either actively (Linington et al., 1988) by immunization with CNS specific antigens (Linington et al., 1993; Mokhtarian et al., 1984; Morris-Downes et al., 2002) in complete Freund's adjuvans or passively (Mokhtarian et al., 1984) by the transfer of activated CNS specific T-cells. Active EAE leads to activation and proliferation of CNS specific T-cells and takes around twelve days until the animals develop first clinical symptoms. In passive EAE the fist clinical symptoms are displayed after three to four days (Table 5).

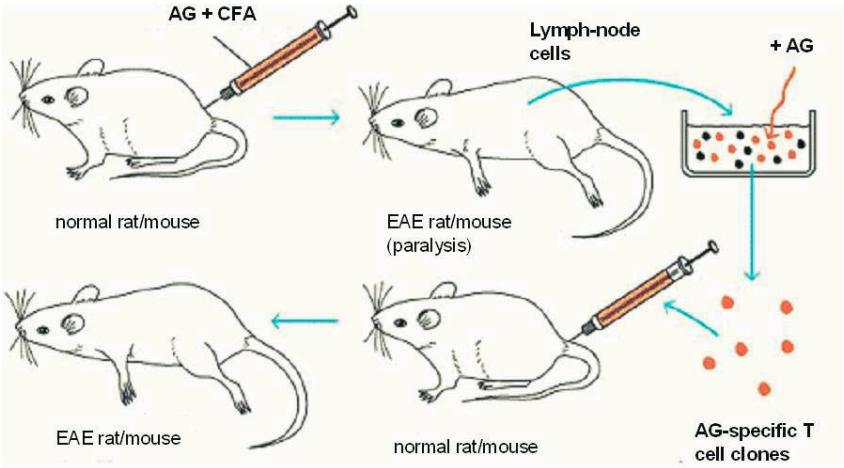

Figure 14 *Active (injection of a CNS antigen in CFA) and passive (transfer of encephalitogenic, activated T-cells) induction of EAE in animal models*

4.2 EAE induction

Materials

- MBP-specific-T-cells
- RPMI-1640 (Lonza, BE12-167F)
- 1 X PBS
    - 150mM NaCl (Merck, 1.06404)
    - 250ml Sörensenbuffer
    - 750ml ddH_2O
- 4% PFA (Merck, 1.04005.1000)
    - 40g PFA dissolved in heated 500ml 0.2M Sörensenbuffer
    - Filled up to 1l with ddH_2O
- 0.2M Sörensenbuffer (pH 7.4)
    - 40mM NaH_2PO_4 (Merck, 1.06346)
    - 160mM Na_2HPO_4 (Merck, 1.06580)

Methods

EAE was induced in Lewis rats (see 4.1), trough intraperitoneal injection of activated MBP-specific-T-cells (3.5-7 X 10^7 cells per animal) in RPMI-1640 medium. The animals were weight daily and the disease development was scored according to Table 5.
The animals were sacrificed when they reached an EAE score of 2 (Table 5) and processed according to the CLARITY protocol below.

Table 5 *shows scores for EAE symptoms.*

Score	Symptomes
0	no clinical symptoms
0,5	partial loss of tail tonus
1	complete loss of tail tonus
2	hind limb weakness
3	hind limb paralysis
4	hind limb and fore limb paralysis
5	death

4.3 Tissue clearing methods

4.3.1 CLARITY (improved)

Materials

- Boric acid (Sigma-Aldrich, B0394-1KG-D)
- Sodium Dodecyl Sulfate (Roth, CN30.4)
- 30% Acrylamide (Roth, 3037.1)
- 2% Bis-acrylamide (Roth, 3039.2)
- VA-044 Initiator Wako (VA-044)
- 16% PFA (Merck, 1.04005.1000)
    - 16g PFA dissolved in heated 50ml 0.2M Sörensenbuffer
    - Filled up to 200ml with ddH_2O
- 10xPBS
    - 1500mM NaCl (Merck, 1.06404)
    - 250ml Sörensenbuffer
    - 750ml ddH_2O
- Hydrogel
    - Acrlamid
    - 10ml Bis-acrylamide
    - 1g VA-044 Initiator
    - 100ml 16% PFA
    - 40ml 10xPBS
    - 210ml dH_2O
- Lipid clearing buffer
    - 46g Boric Acid
    - 160g Sodium Dodecyl Sulfate
    - dH2O fill to 4 L
    - NaOH to pH 8.5
- Heparin-Natrium-25000 (ratiopharm)

Method

A. Transcardial perfusion of mouse and rat brain

The mice and rats used for the CLARITY method were first anesthetized with chloroform and then sacrificed with CO_2. The mice were perfused with 25mL, the rats with 100mL, of 37°C degrees warm PBS (pH 8.5) buffer with 10 units Heparin per milliliter. If there is still blood

left after the given perfusion volume is reached, the perfusion is continued until the PBS becomes colorless. The mice were perfused with 25mL, the rats with 50mL, of ice cold hydrogel solution. The brains were dissected, transferred to a falcon tube and incubated in the hydrogel solution at 4°C for a minimum of one day.

Note: *The perfusion speed should be ~ at 1mL/min to preserve the fine capillary of the blood vessel system. Stiffing of the muscles and a white appearing liver are indicative of successful perfusion.*

B. Tissue embedding by hydrogel polymerization

The falcon tubes with the brains and the hydrogel solution were put for polymerization at 37°C to a water bath for 3-4 hours.

Note: *If acrylamide concentration in the hydrogel solution is lower than described in the materials section the polymerization can take longer or even not solidify.*

The brains were extracted carefully from the fully solidified hydrogel, by rubbing of the hydrogel from the surface and subsequent rolling on a tissue or on Kimwipes. The samples were washed multiple time with 50mL of PBS buffer for 24 hours at room temperature to dialyze the remaining PFA, initiator and monomer. If desired, the tissue sample can be cut into ~1–2-mm blocks immediately after embedding for accelerated clearing.

C. Passive clearing of hydrogel-embedded tissue (passive CLARITY)

The rat samples were cut into thin blocks of ~1mm and transferred to a falcon tube with 50mL of lipid clearing buffer. Buy, gently shaking, the samples were incubated at 50°C for one week.

D. Electrophoretic Tissue Clearing (ETC)

The mouse samples were transferred to ETC chamber (Figure 15 a, b) and the chamber was tightly closed. Plastic mesh sheets were used to fix the orientation of the tissue relative to the electric field direction. For constant circulation of the lipid clearing buffer an KNF

LIQUIPORT® Liquid Pump was used and the electric field was generated by a TTi EX752M Bench Power Supply (Figure 15c). The brains were processed at 27 Watt/0.8 Ampere and 37°C for maximal 3 days.

Note: *The brains should be oriented with the shortest axis parallel to the electric field direction, to maximize the lipid removal. Additionally, it is crucial, that the pH of the lipid clearing buffer is kept above pH8, to minimize the transgenic signal loss.*

The mouse and rat sample were washed multiple times in PBS buffer for one day and then transferred to a RI matching medium until the sample appears transparent.

Note: *If antibody staining was required the samples were processed prior to RI matching as described later in: Tissue staining procedures.*

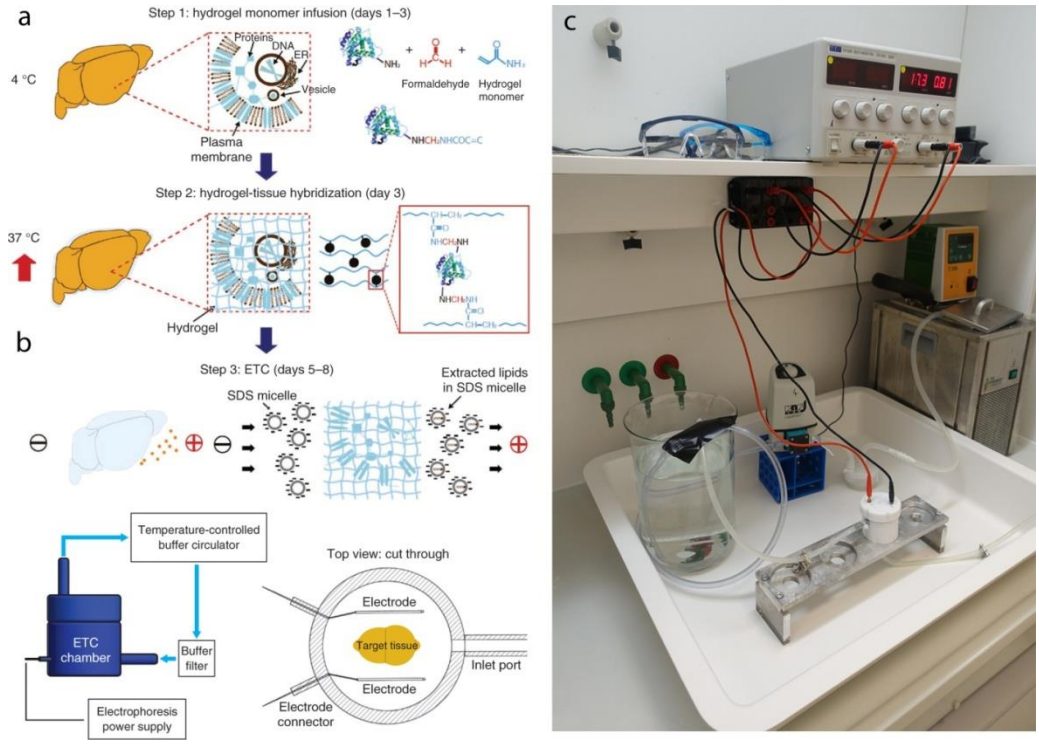

Figure 15 *CLARITY technology and instrumentation. (**a**) Tissue is crosslinked with formaldehyde in the presence of infused hydrogel monomers. Thermally triggered polymerization then results in a hydrogel-tissue hybrid which physically supports tissue structure and chemically incorporates native biomolecules into the hydrogel mesh. (**b**) In electrophoretic tissue clearing (ETC), an electric field is applied across the hybrid immersed in an ionic detergent solution to actively transport ionic micelles into the hybrid and extract membrane lipids out of the tissue, leaving structures and cross-linked biomolecules in place and available for imaging and molecular phenotyping. (**c**) The ETC setup consists of the custom ETC chamber, a temperature-controlled buffer circulator KNF LIQUIPORT® Liquid Pump, a buffer filter (PALL) and a TTi EX752M Bench Power Supply. The sample is electrophoresed by applying ~16 volts to the electrodes. Buffer solution is circulated through the chamber to maintain temperature and the composition of the buffer solution constant throughout the clearing process. The cut-through view (bottom right) shows placement of the hydrogel-embedded tissue in the sample holder located in the middle of the chamber between the two electrodes. The end of each electrode exposed outside the chamber is connected to a power supply. Picture and legend (a,b) are taken and adapted from Chung et al., 2013 and picture (c) was kindle provided by Klaus Becker.*

Troubleshooting

Table 6 *CLARITY troublshooting*

Problem	Possible Cause	Solution
Poor tissue clearing	The two electrodes may be placed too far away from each other	Keep them as close as possible, without touching the sample. This is necessary to create the highest current density to drive tissue clearing
	Overpolymerization of the hydrogel	Do not leave the sample in the monomer solution (at 37 °C) for more than 5–6 h. If the samples are polymerized overnight, this will make tissue clearing and staining very difficult
Tissue damage during clearing: black deposits on samples and electrodes	Black deposits will form on the cathode over time and will gradually start to transfer to the tissue surface, if left unattended	The electrodes can be easily cleaned by reversing the voltage polarity, putting them in a NaCl or KCl solution and running the power high for 3 minutes
Tissue damage during clearing: Sample burned or turned yellow	High temperature (resulting from higher current and/or insufficient heat dissipation due to low flow rate) will cause yellowness or may even burn or melt the samples	Individual users must determine the optimal combination of voltage, temperature and flow rate settings on the basis of the sample properties and chamber design
Loss offluorescence	High temperature or voltage can quench fluorescence, as can high acidity	It is crucial to maintain the temperature at 37 °C and the pH above pH8

4.2.2 3-DISCO (adapted)

Materials

- 16% PFA (Merck, 1.04005.1000)
    - 16g PFA dissolved in heated 50ml 0.2M Sörensenbuffer
    - Filled up to 200ml with ddH_2O
- 10xPBS
    - 1500mM NaCl (Merck, 1.06404)
    - 250ml Sörensenbuffer
        - 750ml ddH_2O
        - NaOH to pH 8.2
- Heparin-Natrium-25000 (Ratiopharm)
- Tetrahydrofuran (THF) (Roth, CP82.1)
- Dibenzyl ether (DBE) (Millipore, 103-50-4)

Method

A. Transcardial perfusion of mouse brain

The mice used for the 3-DISCO method were first anesthetized with chloroform and then sacrificed with CO_2. The mice were perfused with 25mL, of 37°C degrees warm PBS (pH 8.2) buffer with 10 units Heparin per milliliter. If there is still blood left after the given perfusion volume is reached, the perfusion is continued until the PBS becomes colorless. The brains were dissected, transferred to a falcon tube and incubated in 4%PFA solution at 4°C for one day.

B. Tissue dehydration

The brains were washed three times for 20 minutes in PBS and each brain was transferred into a glass vial and 10mL of 30% THF in PBS was added. The samples were incubated on a shaking table for 3 hours at 4°C. Then, the solution was discarded and replaced by 10mL of 50% THF in PBS. The sample were again incubated on a shaking table for 3 hours at 4°C. The solution was discarded and replaced by 10mL of 70% THF in PBS. The sample were incubated on a shaking table over night at 4°C.

The solution was discarded and replaced by 10mL of 80% THF in dH_2O. The samples were incubated on a shaking table for 3 hours at 4°C. Further, the solution was discarded and replaced by 10mL of 90% THF in dH_2O. The sample were again incubated on a shaking table for 3 hours at 4°C. The solution was discarded and replaced by 10mL of 96% THF in dH_2O. The sample were incubated on a shaking table over night at 4°C.

Then, the samples were transferred in pure THF and were incubated on a shaking table at 4°C. The samples were kept under this conditions and pure THF was change twice a day for overall three days. During this time the samples should be completely dehydrated.

Note: *If antibody staining was required the samples were processed prior to RI matching as described later in: Tissue staining procedures.*

C. RI matching with DBE

The dehydrated brains were incubated in increasing DBE concentrations in THF (50%, 80%, 96% and 100% DBE). Each incubation step was ~60 minutes on a shaking table at 4°C. The solution was discarded after each step. To reach the final transparency the samples were incubated for two additional days in DBE on a shaking table at 4°C.

Note: *If peroxide concentration is minimized in THF and DBE and if the brains are stored in DBE at 4°C, the transgenic fluorescence signal can be maintained longer than described in table 1.*

Troubleshooting

Table 7 *3-DISCO troublshooting*

Problem	Possible Cause	Solution
The tissue does not get transparent	Blood is retained in the tissue	Use proper fixation methods (cardiac perfusion) to wash out the blood from the tissue.
Weak or no detectable fluorescence signal	Insufficient clearing	Extend the incubation time of the clearing steps, especially the DBE step
	Excessive clearing	Reduce the incubation times of the clearing steps, especially the final DBE step
Weak or no detectable fluorescence signal	Low fluorescence expression (if transgenic models are used for labeling)	Check whether the signal could be detected before clearing by making tissue sections and imaging them without clearing. If the signal is not detectable, use another transgenic line or labeling method to obtain a brighter signal
	Insufficient laser power	Increase the power of the imaging laser. Increase the exposure time of the image capture
	Peroxidized clearing chemicals	Peroxide contaminations in THF or DBE can diminish fluorescent signal even at very low concentrations. Check peroxide concentrations using peroxide test strips. Use fresh reagents or remove excessive peroxide as described

4.3 Procedure for generating and purifying fluorophore labeled F(ab')2 fragments

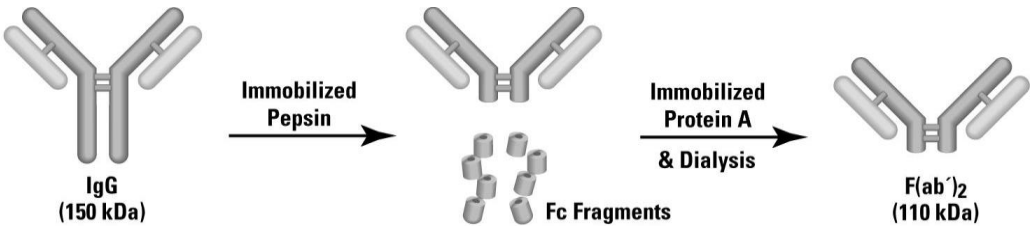

Figure 16 *Schematic for preparing F(ab´)2 using Immobilized Pepsin and Protein A.*

Materials

-GFAP antibody (polyclona-rabbit) (Dako Z0334)
- Pierce™ F(ab')2 Preparation Kit (Thermo Fisher Scientific 44988)

- Immobilized Pepsin, 1.25mL settled resin, contains 2-3mg (> 6000 units) of pepsin per milliliter of settled resin; support is 6% crosslinked beaded agarose supplied as a 50% slurry in 50% glycerol, 0.1M sodium acetate, pH 4.4; 0.05% sodium azide
- NAb™ Protein A Plus Spin Column, 1mL, 1 each, binding capacity: ≥ 34mg of human IgG per column
- BupH™ Phosphate Buffered Saline, 2 packs, makes 1L of 0.1M sodium phosphate, 0.15M sodium chloride; pH 7.2
- IgG Elution Buffer, 120mL, pH 2.8, contains primary amine
- Spin Columns, 10 each, 0.8mL columns with 10 caps and 11 bottom plugs Microcentrifuge Tubes, 30 each, 2.0mL collection tubes
- Digestion Buffer, 120mL, 20mM sodium acetate, pH 4.4; 0.05% sodium azide
- Zeba™ Spin Desalting Columns, 2mL, 10 each, for 200-700mL samples

Storage: Upon receipt store kit at 4-8°C. Kit.

Method

A. Immobilized Pepsin Equilibration

The Pepsin vial was gently swirled to obtain an even suspension. The spin column frit was seated with an inverted 200µL pipette tip. Afterwards the bottom tab from a 0.8mL spin column was twisted off and placed into a 2mL microcentrifuge tube. By using a cutted pipette tip 250µL of the 50% slurry (i.e. 125µL of settled resin) were placed in a 0.8mL spin column and centrifuged at 5000 x g for 1 minute. Then the buffer was discarded and the resin was washed with 0.5mL of Digestion buffer. The column was again centrifuged at 5000 x g. After discarding the buffer the bottom of the spin column was caped with a rubber cap.

B. IgG Sample Preparation

The bottom of a Zeba Spin Deasalting Column was twisted off and the cap was loosen. Afterwards the column was placed in a 15mL collection tube and centrifuged at 1000 x g for 2 minutes to remove storage solution. Then, 1mL of Digestion Buffer was added to the column and the column was centrifuged again at 1000 x g for 2 minutes to remove the buffer. This procedure was repeated three additional times and the buffer was discarded from the collection tube. The column was placed in a new collection tube, the cap was removed and 0.5mL of the GFAP antibody was slowly applied to the center of the compacted resin bed. The cap was replaced and the column was centrifuged at 1000 x g for 2 minutes to collect the sample. After the column was used it was discarded.

Note: *If IgG sample is 0.5-8mg/mL (i.e., 250µg to 4mg), no further preparation is necessary. If sample volume is less than 0.5mL, add Digestion Buffer to a final volume of 0.5mL.*

C. Fragment Generation

0.5mL of the prepared GFAP IgG were added to the spin column containing the equilibrated Immobilized Pepsin (Section A) and the top cap and the bottom plug are place on the spin column. Afterwards, the digestion reaction was incubated for one and a half hours on a shacking table at 37°C. The constant mixing was maintained during the incubation. Then, the bottom cap was removed and the column was placed into a 2mL microcentrifuge tube and centrifuged at 5000 x g for 1 minute to separate digest from Immobilized Pepsin. The resin

was washed with 0.5mL of PBS and centrifuged at 5000 x g for 1 minute. The washing was repeated once. Both washed fraction were added to the digested antibody. The total sample volume should be 1.5mL. The Immobilized Pepsin was discarded.

D. F(ab')$_2$ Purification

The NAb Protein A Plus Column, the PBS and the IgG Elution Buffer were equilibrated to room temperature. The top cap of the NAb Protein A Plus Column was loosen and the bottom cap was removed. Then, the column was placed in a 15mL collection tube and centrifuged at 1000 x g for 1 minute to remove storage solution (contains 0.02% sodium azide) and the flow-through was discarded. The column was equilibrated by adding 2mL of PBS and centrifuged for 1 minute and the flow-through was discarded. This step was repeted once. The bottom of the column was caped with a rubber cap and the 1.5mL of the sample were applied to the column. The resin and the sample were resuspended by inversion. Afterwards, the resin-sample mixture was incubated at room temperature by end-over-end mixing for 10 minutes. After loosen the top cap and removing the bottom cap the column was placed in an new 15mL collection tube and centrifuged for 1 minute. The flow-through was saved as this fraction contains F(ab')2 and Fc fragments that are too small to bind to Protein A.

Note: *For optimal recovery, the column can be washed with 1mL of PBS. Centrifuged for 1 minute and the flow-through can be collected. This can be repeated and the fractions can be combined with the F(ab')2 fraction from above.*

The fractions are then concentrated trough centrifugation in an 10kDa cutoff Amicon spin filter tube to a volume between 300-500µL and the protein concentration is measured by using the absorbance at 280nm in a NanoDrop. Thereby a extinction coefficient of 1.4 is used assuming a complete GFAP-IgG digestion.

E. Regeneration of the Immobilized NAb Protein A Plus Spin Column

3mL of IgG Elution Buffer was applied to the NAb Protein A Plus Spin Colum and centrifuged a 1000 x g for 1 minute. This was repeated two times and the flow-through was discarded.

Then 3mL of PBS was added to the column and centrifuged for 1 minute. For storage 3mL of 0.02% sodium azide in PBS was added to the column and the column was stored upright at 4°C.

Troubleshooting

Table 7 *F(ab')2 protocol troublshooting*

Problem	Possible Cause	Solution
Low amounts of $F(ab')_2$ produced as determined by non-reducing SDS-PAGE	IgG sample was not in Digestion Buffer	Dialyze or buffer exchange IgG into Digestion Buffer, or decrease the Digestion Buffer pH to 3-4.3 [note that decreasing the pH might increase the $F(ab')_2$ amount produced but can reduce its immunoreactivity]
	Sample loading buffer contains reducing reagent	Use SDS loading buffer that does not contain β-mercaptoethanol, DTT or TCEP
	Resin was not equilibrated in Digestion Buffer before adding IgG	Wash resin with 0.5mL of Digestion Buffer before adding IgG sample
	Sample is goat or mouse IgG	Reduce IgG concentration and increase digestion time to 8 hours
	Some mouse IgG are resistant to pepsin cleavage	Use the Pierce IgG Fab and $F(ab')_2$ Preparation Kit (Product No. 44980 or 44680)
	Sample contains protein other than IgG (i.e., BSA), which can increase digestion time	Remove BSA with the Pierce Antibody Clean-up Kit (Product No. 44600)
$F(ab')_2$ has low immunoreactivity	Sample digested for too long	Reduce digestion time; do not exceed 8 hours
	The low pH of Digestion Buffer decreased $F(ab')_2$ activity	Use the Pierce IgG Fab and $F(ab')_2$ Preparation Kit
Low $F(ab')_2$ recovery	Incomplete washing of the pepsin resin	Two 500µL washes of PBS are required for maximum recovery
A portion of undigested IgG does not bind to Protein A	Sample is goat or mouse IgG	Goat IgG binds weakly to Protein A, so try an alternative purification method such as ion-exchange
		Dilute sample in Pierce Protein A Binding Buffer (Product No. 21001) before adding to the Protein A column

The fluorophre conjugation to the F(ab')2 parts are performed by Florain Kelber, MSc from our cooperation partner, the Huppa Laboratory.

F. Conjugation of fluorophore to the GFAP-F(ab')2 part

The GFAP-F(ab')2 sample was labeled with the Alexa Fluorophores-(AF)-555 succinimidly ester. The sample was incubated with a 6M excess of AF-555 and a 0.1M $NaHCO_3$ for 10 minutes at room temperature.

Note: *The incubation time is dependent on the sample and should be chosen, so that each antibody fragment is labeled with one fluorochrome. To determine if the reaction was sufficient the degree of labeling should be calculated (see below).*

The unbound fluorophores are then separated by Size-exclusion chromatography (SEC) and the fractions are examined with an ultraviolet (UV) detector. The fractions containing the GFAP-F(ab')2-AF555 fragments are pooled and concentrated trough centrifugation in an 10kDa cutoff Amicon spin filter tube to a final volume between 300-500µL.

G. Measurements and calculations to determine the degree of labeling (DOL)

Table 8 *Spectral characteristics of Alexa Fluor 555 dye*

Dye	Molecular Weight	λ_{max}*	Em*	ε †	CF_{280} ‡	CF_{260} §
Alexa Fluor® 555	~1250	555	565	150,000	0.08	0.08

** Fluorescence absorbance and emission maxima, in nm, conjugated to an IgG antibody. † Extinction coefficient at λmax in cm-1M-1. ‡ Correction factor for absorption readings (A280) at 280 nm; i.e., A280,actual = A280,observed – (CF280 × λmax). § Correction factor for absorbance readings (A260) at 260 nm; i.e., A260,actual = A260,observed – (CF260 × λmax).*

The absorbance at 280nm (A_{280}) and at the λ_{max} for the dye (A_{max}) of the protein-dye conjugate was measured. This is important to determine the concentration of the protein in mg/mL with the following formula:

$$A_{protein} = (A_{280} - A_{max} \times CF)/1.4$$

For IgG a corrected value of 1.4 is used in this formula, assuming that 1.4 $A_{protein}$ units= 1mg/mL

The DOL is calculated according to following formula:

$$DOL = \frac{A_{max} \times MW}{[protein] \times \varepsilon_{dye}}$$

where MW = the molecular weight of protein (i.e. IgG= 15000g/mol; F(ab')2= 11000g/mol), ε_{dye} = the extinction coefficient of the dye at its absorbance maximum, and the protein concentration is in mg/mL.

4.4 Tissue staining procedures

Table 9 *list of used antibodies*

Primary Antibody	**Antibody Type**	**Target**	**Dilution**	**Pre treatment**	**Source**
GFAP	Rabbit, pc^	filaments of mature astrocytes	1:1000	SDS/boric acid pH 8,5 or various iDISCO pre treatments	DAKO Z0334
Ox6	Mouse, mc*	Cytoplasmic granules of cytolytic T-lymphocytes and natural killer cells	1:50	SDS/boric acid pH 8,5	Abcan, ab4059
SMI-31	Mouse, mc*	phosphorylated epitope in extensively phosphorylated neurofilament	1:100	SDS/boric acid pH 8,5	Biocompare, SMI-31R-500
PLP	Rabbit, pc^	Proteolipid Protein	1:250	SDS/boric acid pH 8,5	Sara Piddlesten
Iba-1	Rabbit, pc^	microglial and macrophages ionized Ca2+-binding protein	1:3000	SDS/boric acid pH 8,5	Wako Pure Chemical Industries, 019-19-741
fluorophore coupled secondary antibodies			**Dilution**	**Incubation**	**Source**
Hsαm#DL488			1:100	Dako diluent	Abcam, ab96879
dαR+Cy3			1:100	Dako diluent	Abcam, ab6939
fluorophore coupled F(ab')2 parts			**Dilution**	**Incubation**	**Source**
GFAP-F(ab')2-AF555			1:50 Or 1:00	Dako diluent	Self made

mc*=monoclonal; pc^=polyclonal; #horse anti mouse; +donkey anti rabbit

Immunohistochemistry (IHC) uses specific antibodies that are directed against the epitopes from proteins of interest. A secondary antibody that is coupled to a fluophore is used to detect the first or so called primary antibody and to visualize the construct.

If working with thick tissue very long incubation times are required to acquire deep tissue penetration of the antibodies. Therefore, small primary antibodies or antibody parts, i.e. F(ab')2 parts, can be directly coupled to a fluorophore. That shortens the incubation time, by making the incubation step with the secondary antibodies redundant.

4.4.1 Staining of hydrogel embedded thin tissue sections

Materials

- Coverslip 21x26mm (Carl Roth, H8762)
- Blu-Tack (Bostik)
- 0.2M Sörensenbuffer (pH 7.4)
    - 40mM NaH_2PO_4 (Merck, 1.06346)
    - 160mM Na_2HPO_4 (Merck, 1.06580)
- 1 X PBS
    - 150mM NaCl (Merck, 1.06404)
    - 250ml Sörensenbuffer
    - 750ml ddH_2O
- Lipid clearing buffer
        - 46g Boric Acid
        - 160g Sodium Dodecyl Sulfate
        - dH_2O fill to 4 L
        - NaOH to pH 8.5
- DAKO diluents (DAKO, S2022)
- DAKO buffer (DAKO, S3006)
- Primary and secondary antibodies (Table 8)
- 2,2'-Thiodiethanol (Sigma-Aldrich 166782-500G)

Methods

One mm tick hydrogel embedded EAE-rat sections were incubated in 50mL of lipid clearing buffer on a shaking table for one week at 37°C. Thereafter, the lipid clearing buffer was discarded and the sections were washed on a shaking table for one day in PBS at room temperature. The nonspecific binding sites were blocked for one day with DAKO diluent in a humid chamber at room temperature.
The sections were incubated after the blocking step on a shaking table for one week with primary antibodies in DAKO diluent buffer at 4°C. The samples were washed for one day in PBS. Afterwards, the sections were incubated with the secondary antibodies on a shaking table for another week in DAKO buffer at 4°C. The samples were washed one a shaking table in PBS for one day at room temperature. Finally, the RI of the sections was matched to 1.45 with TDE and after 24 hours a sufficient transparency was reached.

The sections were mounted as followed: A thick border of blue tack was created on a glass slide and the tissue was placed in the middle of the pool. The pool was filled with TDE and covered with an glass cover slip.

Tissue sections were examined with an Leica TCS SP5 LASAF confocal microscope (Leica Microsystems, CMS-GmbH, Germany).

4.4.2 Staining procedure with microwave

Materials

- DAKO diluents (DAKO, S2022)
- DAKO buffer (DAKO, S3006)
- Primary and secondary antibodies (Table 8)
- Microwave (CLA Tronic)
- Gelto
    - 6g glycerine (Gibco BRL, 15514-011)
    - 2,4g Mowiol (CalbioChem, 475904)
    - 12ml Tris 0,2M pH 8,5 (AppliChem, A1379)

- 6ml dH2O
- Stirred for 10 minutes at 50°C, centrifuge at 5000g for 15 minutes

– 0,1M Gallate (Sigma, P3130) in Geltol

Astrocyte covered cell culture glass plate were provided by Bleranda Zeka, MSc from our cooperation partner, the Lassmann Laboratory.

Method

All steps were performed in a commercial microwave. The temperature was controlled by dry ice (Figure 17). The microwave power settings are expressed as continuous power in watts (W). Time switch interrupted microwave irradiation cycles were used for primary and secondary antibody incubations.

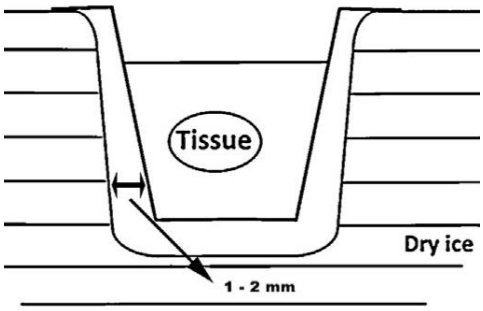

Figure 17 *A schematic drawing that shows the setup for using dry ice facilitated cooling of tissue samples during microwave irradiation. In a small plastic box crushed powder dry ice was filled to the top. Indentations into the dry ice were made using the bottom of the incubation cup. The cups were placed into the dry ice so there was about 1–2 mm space between the edge of the cup and the dry ice. Picture and legend are taken and adapted from Owens et al., 2013*

The cell culture plates were incubated with the primary antibodies in Dako diluent for 6 minutes at 150W in the microwave. After 1 minute of cooling phase the microwave was switched on again for 6 minutes at 150W. Then, the samples were rinsed in PBS.

Afterwards, the cell culture plates were incubated with the secondary antibodies in Dako buffer for 6 minutes at 150W in the microwave. After 1 minute of cooling phase, the microwave was switched on again for 6 minutes at 150W. Afterwards, the samples were rinsed in dH_2O and mounted on a glass slide with Gallate-Geltol.

Samples were examined with an Leica TCS SP5 LASAF confocal microscope (Leica Microsystems, CMS-GmbH, Germany).

4.4.3 Staining of adult mouse hemispheres with iDISCO and iDISCO adaptations

Materials

- 16% PFA (Merck, 1.04005.1000)
    - 16g PFA dissolved in heated 50ml 0.2M Sörensenbuffer
    - Filled up to 200ml with ddH_2O
- 10xPBS
    - 1500mM NaCl (Merck, 1.06404)
    - 250ml Sörensenbuffer
        - 750ml ddH_2O
        - NaOH to pH 8.2
- Heparin-Natrium 25000
- Glycine (Roth, 3908.2)
- Methanol (VWR International GmbH, 20847.307)
- Tetrahydrofuran (THF) (Roth, CP82.1)
- Dibenzyl ether (DBE) (Millipore, 103-50-4)
- H_2O_2 (Roth, CP26.1)
- DMSO (Merck, ME328)
- Triton-X 100 (Roth, 3051.2)
- Tween 20 (Roth, 9127.2)
- NP 40 (Sigma, 56741-250ML-F)
- Deoxylate (Sigma Aldrich, D6750-25G)
- FCS (Biochrom S01115)
- PBST
    - 1xPBS
    - 0,2% Triton-X 100
- Solution 1
    - PBST
    - 20%DMSO
- Solution 2
    - PBST
    - 0,1% Tween 20
    - 0,1% deoxycholate
    - 0,1% NP 40
    - 20% DMSO

- Blocking serum
    - PBST
    - 10% DMSO
    - 6% FCS serum
- PTwH
    - 1xPBS
    - 0,2% Tween 20
    - 10mg/ml Heparin
- Solution 3
    - PTwH
    - 5%DMSO
    - 3% FCS serum

Method

A. Transcardial perfusion of mouse brain

The mice used for the iDISCO method were first anesthetized with chloroform and then sacrificed with CO_2. The mice were perfused with 25mL, of 37°C degrees warm PBS (pH 8.2) buffer with 10 units Heparin per milliliter. If there is still blood left after the given perfusion volume is reached, the perfusion is continued until the PBS becomes colorless. The brains were dissected, transferred to a falcon tube and incubated in 4%PFA solution at 4°C for one day.

B. Different tissue pretreatment approaches for IHC

With Methanol

The brains were washed three times for 20 minutes in PBS and each brain was transferred into a glass vial and 10mL of 50% methanol in PBS was added. The samples were incubated on a shaking table for 1 hours at 4°C. Then the solution was discarded and replaced by 10mL of 80% methanol in dH_2O. The sample were again incubated on a shaking table for 1 hours at 4°C. The solution was discarded and replaced by 10mL of 100% methanol and incubated on a shaking table for 1 hours at 4°C. The last step was repeated once. Then, the sample were

incubated on a shaking table in 5%H_2O_2 in DMSO/methanol (1 vol 30% H2O2/ 1 vol DMSO/ 4 vol methanol, ice cold) over night at 4°C.

The brains were washed two time on a shaking table with 100% methanol for 1 hour at 4°C. Afterword the brains were placed in 20% DMSO in methanol for 1 hour at 4°C. Then, the rehydration process was started, by putting the samples in 80% methanol for 1 hour and then in 50% methanol for another hour at 4°C. The brains were washed twice in PBS for 1 hour. Finally, the samples were put for two hours in PBST prior to IHC.

With THF

The brains were washed three times for 20 minutes in PBS and each brain was transferred into a glass vial and 10mL of 50% THF in PBS was added. The samples were incubated on a shaking table for 1 hours at 4°C. Then the solution was discarded and replaced by 10mL of 80% THF in dH_2O. The sample were again incubated on a shaking table for 1 hours at 4°C. The solution was discarded and replaced by 10mL of 100% THF and incubated on a shaking table for 1 hours at 4°C. The last step was repeated once. Then, the sample were incubated on a shaking table in 80% THF/ 0,2% Triton-X 100 over night at 4°C.

The brains were washed two time on a shaking table with 80% THF/ 0,2% Triton-X 100 for 1 hour at 4°C. Then, the rehydration process was started, by putting the samples in 80% THF for 1 hour and then in 50% THF for another hour at 4°C. The brains were washed twice in PBS for 1 hour at 4°C. Finally, the samples were put for two hours in PBST prior to IHC.

With detergents

The brains were washed two times for 1 hour in PBS and each brain was transferred into a glass vial and 10mL of PBST was added. The samples were incubated on a shaking table for 1 hours at 4°C. This step was repeated once. Afterwards, the sample were incubated on a shaking table in solution 1 over night at 37°C.

The solution 1 was discarded and solution 2 was added. Then, the brains were incubate on a shaking table over night at 37°C.

Finally, the samples were washed two time with PBST for 1 hour prior to IHC

C. IHC of differently pretreated brains

Pretreated samples were incubated on a shaking table in PBST/ 20% DMSO/ 0.3 M glycine at 37°C over night. Then, they were blocked in PBST/ 10% DMSO/6% Donkey Serum at 37°C for 1 day. The brains were washed twice in PTwH for 1 hour. Finally, the samples were incubated on a shaking table with GFAP-F(ab')2-AF555 antibody fragments in PTwH/ 5% DMSO/ 3% FCS serum for 9 days at 37°C.

D. Tissue clearing

The tissue was further processed according to the 3-DISCO protocol above.

4.4.4 Imaging of large specimens

The specimens were illuminated with a planar sheet of light, formed ether by cylindrical lenses and slit aperture (Figure 18) or

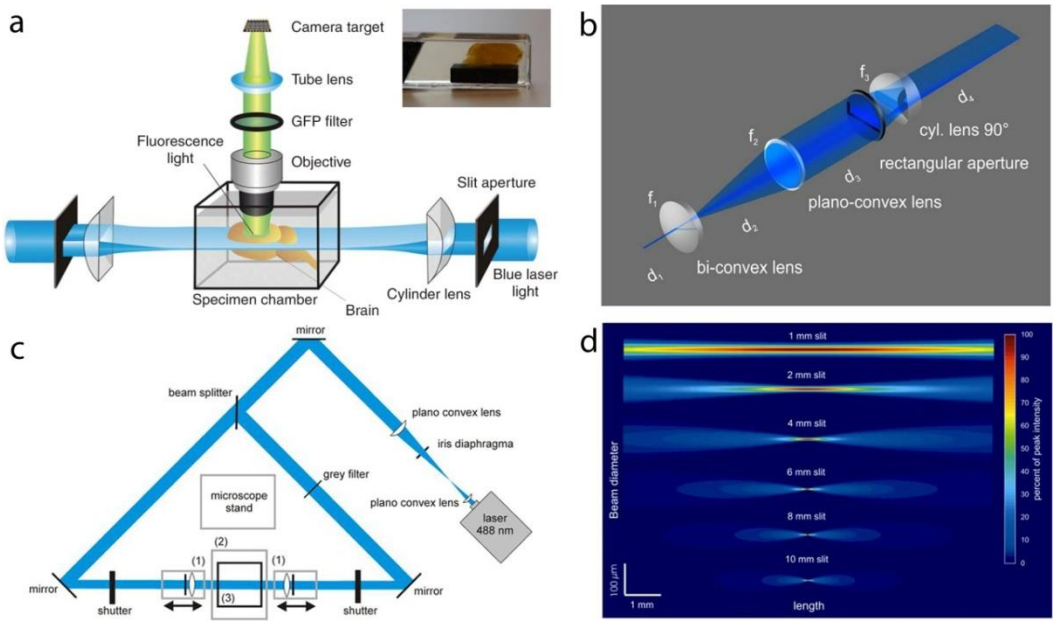

Figure 18 Standard Ultramicroscopy ***(a)*** *3-DISCO cleared samples were recorded in a chamber filled with dibenzyl ether (DBE), RI 1.56. CLARITY cleared sample were recorded in a cuvette (right upper corner) filled with BrainClear (**b**) Light sheet generating optics and slit aperture. (**c**) Optical setup for standard Ultramicroscopy.(**b**) light sheet thickness in relation to slit aperture. Pictures are kindly provide by Saiedeh Saghafi*

by two condensor aspheric lenses, powell lenses and two aspheric cylindrical lenses (Figure 19).

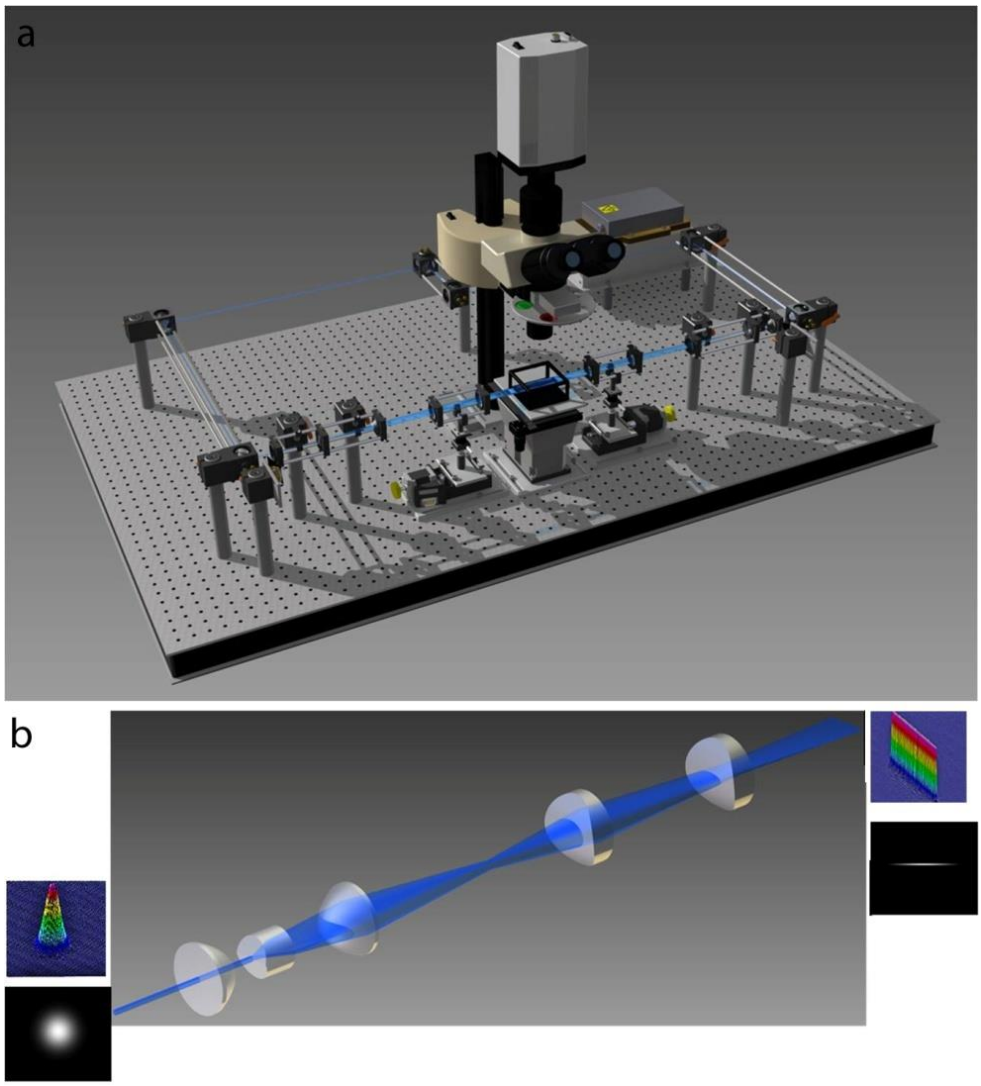

Figure 19 High resolution a*spheric Ultramicroscopy system. (**a**) Blue line is indicating the laser pathway. (**b**) Light sheet generating optics: two condensor aspheric lenses, powell lenses and two aspheric cylindrical lenses. Input Gaussian laser beam (left down corner), output thin light sheet (upper right corner) . Pictures were taken from Saghafi et al., 2014.*

For fluorescence observation an argon-ion laser (488 nm Sapphire Laser, 200 mW) was used. The images were obtained with objectives corrected for RI 1.45 or RI 1.56 (Figure 20). The images were recorded with an sCMOS camera (Andor technology, neo 2560 x 2160 pixels) and the obtained optical section were processed and 3 D reconstructed with the AMIRA (FEI company) software.

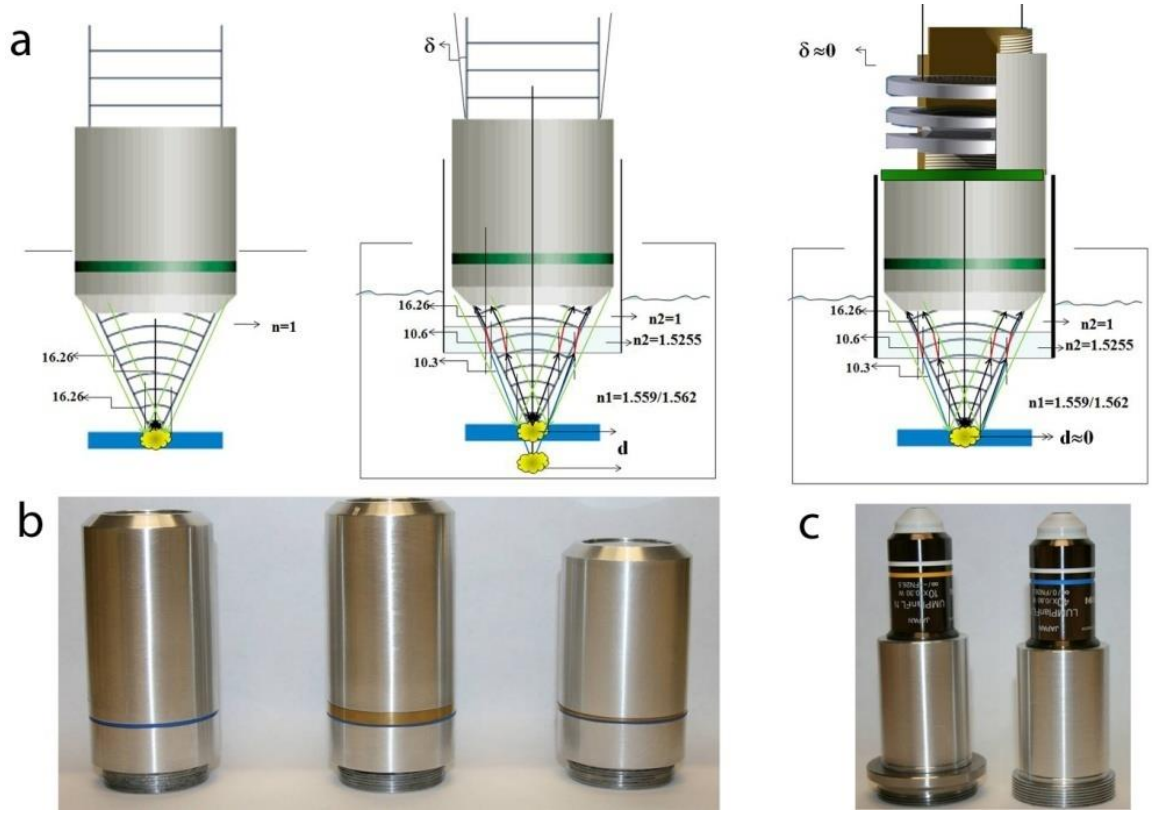

Figure 20 *CLARITY or 3-DISCO corrected objectives. (**a**) Refractive index mismatch leads to considerable alteration of the axial dimension (middle picture). True dimensions must be restored by rescaling the Z-axis of the image stack. Corrected-objectives for RI 1.45 or RI 1.56 are designed using combination of aberration-corrected lenses that corrects the d-distance and δ-angle (left picture). (**b**) Corrected objectives in immersion cap (from left to right): 2X N.A.0.14, 4X N.A. 0.28 (Working distance 10mm) and 20X N.A. 0.45 (Working distance 5mm). (**c**) Corrected water immersion objectives for CLARITY: 10X N.A. 0.3 and 40X N.A.0.8 (Working distance 3mm). Pictures were kindly provided by Hans Ulrich Dodt.*

5. Results

5.1 Mouse brain clearing with optimized CLARITY protocol

All CLARITY procedures have been performed according to the protocols, described in the materials and method section.

During the electrophoretic tissue clearing (ETC) process, pH of the lipid removing buffer decreases gradually, from 8.5. To test the effect of lower pH on the brain tissue and fluorescent signal, the lipids from brains were removed using the ETC-buffer with different pH-values. The brains, where the pH of the SDS/boric acid buffer was dropped to 7.5 during the ETC procedure have shown major loss of the fluorescent signal but no effect on the tissue transparency, in comparison to the brains, where pH of the lipid removing solution was kept above 8 (Figure 21).

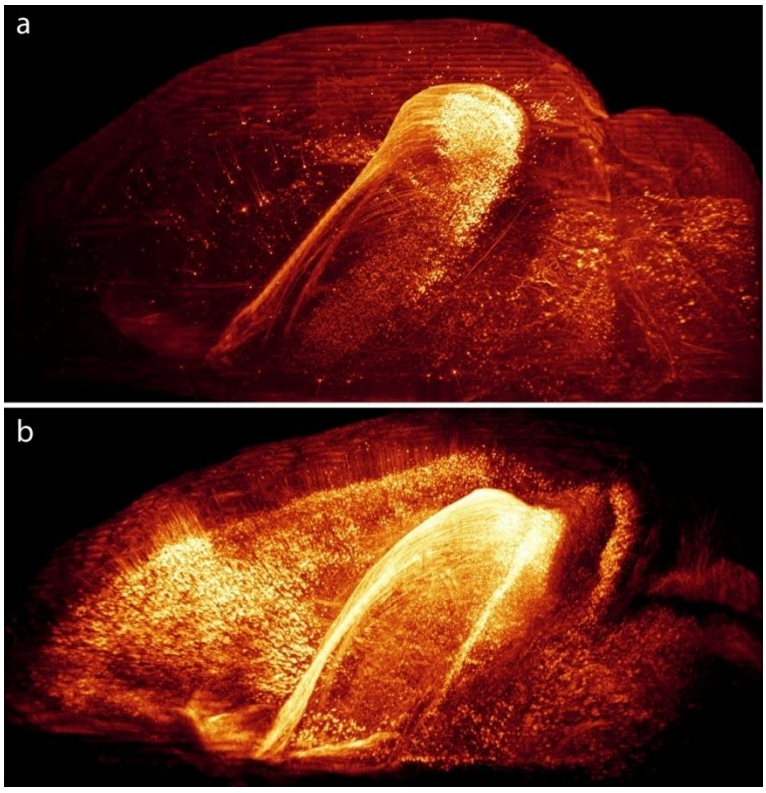

Figure 21 *Electrophoretic tissue clearing (ETC) performed on hydrogel embedded adult TH1-GFP-M mouse brains. The refraction index (RI) was matched with BrainClear (**a**) Hemisphere showing the effect on fluorescence of pH dropping below 8 (in this case pH 7.6). (**b**) Control hemisphere with pH kept above 8.*

Various refractive index matching- media have different properties regarding reachable sample transparency, tissue storage and fluorescent signal preservation. The RI matching media Histodenz (Tomer et al., 2014; Yang et al., 2014) that has shown the best results for hydrogel embedded samples so far, was compared with BrainClear - RI matching medium developed in our laboratory. To examine the optical properties (Figure 22) and

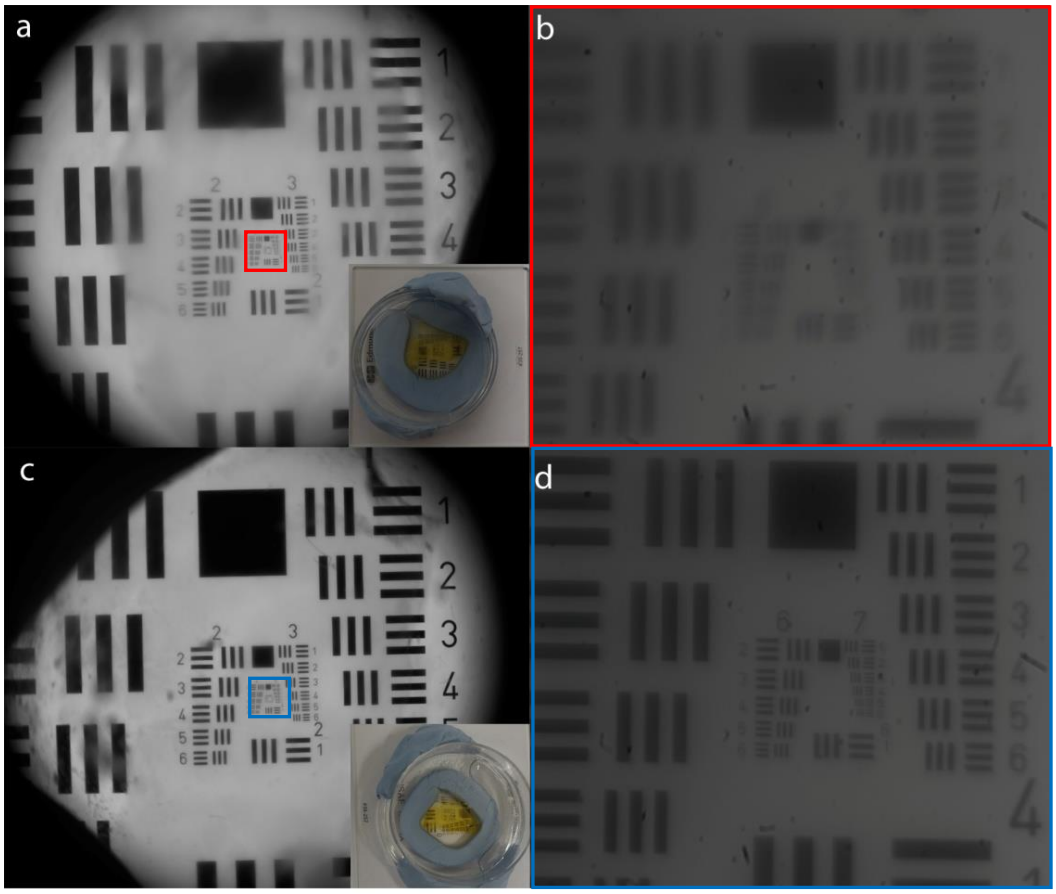

Figure 22 *Optical properties from hemispheres of one brain with different RI matching media.(**a**) Histodenz cleared hemisphere (right lower corner shows true color image), picture obtained with 1,2x magnification. (**b**) Red boxed region in (a), pictures obtained with 10x objective. (**c**) BrainClear cleared hemisphere (right lower corner shows true color image), picture obtained with 1,2x magnification. (**d**) Blue boxed region in (c), pictures obtained with 10x objective.*

fluorescent signal preservation (Figure 23) brains were treated according to standard ETC procedure. Each brain was cut afterwards into two hemispheres and each half of the brain was incubated in one of the above mentioned refraction index matching media. The hemispheres of every brain were compared to each other after reaching sufficient transparency. In five different brains, BrainClear has shown superior fluorescence preservation and better transparency than Histodenz.

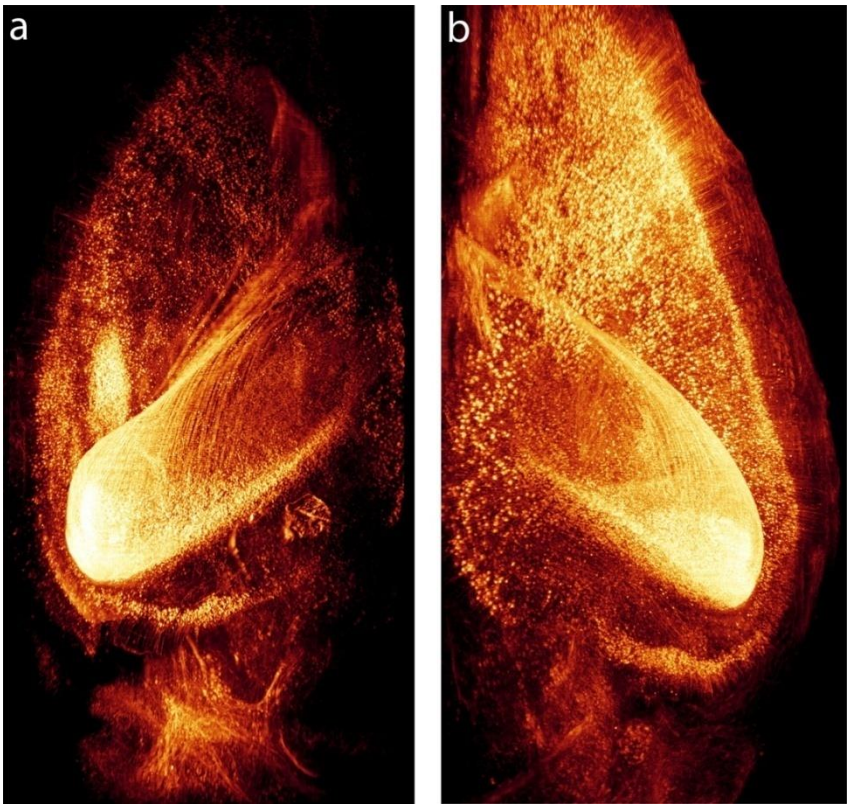

Figure 23 *Fluorescence preservation from hemispheres of one brain with different RI matching media. ETC was performed on hydrogel embedded adult TH1-GFP-M mouse brains (**a**) RI was matched with Histodenz. (**b**) RI was matched with BrainClear.*

To test the long term storage properties of the BrainClear, samples were recorded after reaching adequate transparency at first, and later they were recorded again after seven months. No significant difference could be detected in the transgenic GFP signal (Figure 24).

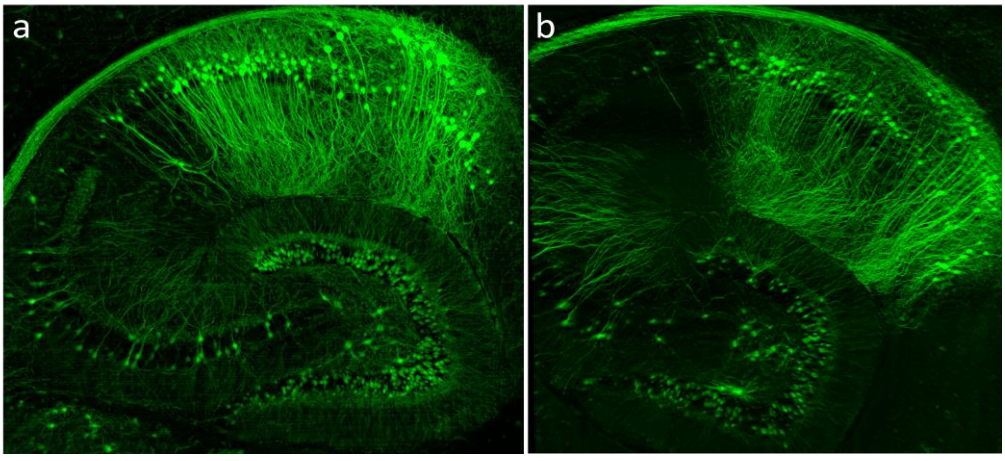

Figure 24 *Storage properties of BrainClear. (**a**) Hippocampus of adult mouse brain was recorded 3 days after RI incubation. (**b**) Recording of same hippocampus after seven months of storage in BrainClear.*

5.2 Immunohistochemistry (IHC) of passive CLARITY cleared thick rat sections

Experimental autoimmune encephalomyelitis (EAE) rat brain sections were processed according to the staining protocol for hydrogel embedded thin tissue sections.

To test the applicability of immunohistochemistry (IHC) on hydrogel embedded CLARITY cleared specimens, double staining was performed on 1mm thick EAE-rat sections with different antibodies (Figure 25). In addition, I tried to visualize in 3D the neuronal structures and activated immune system.

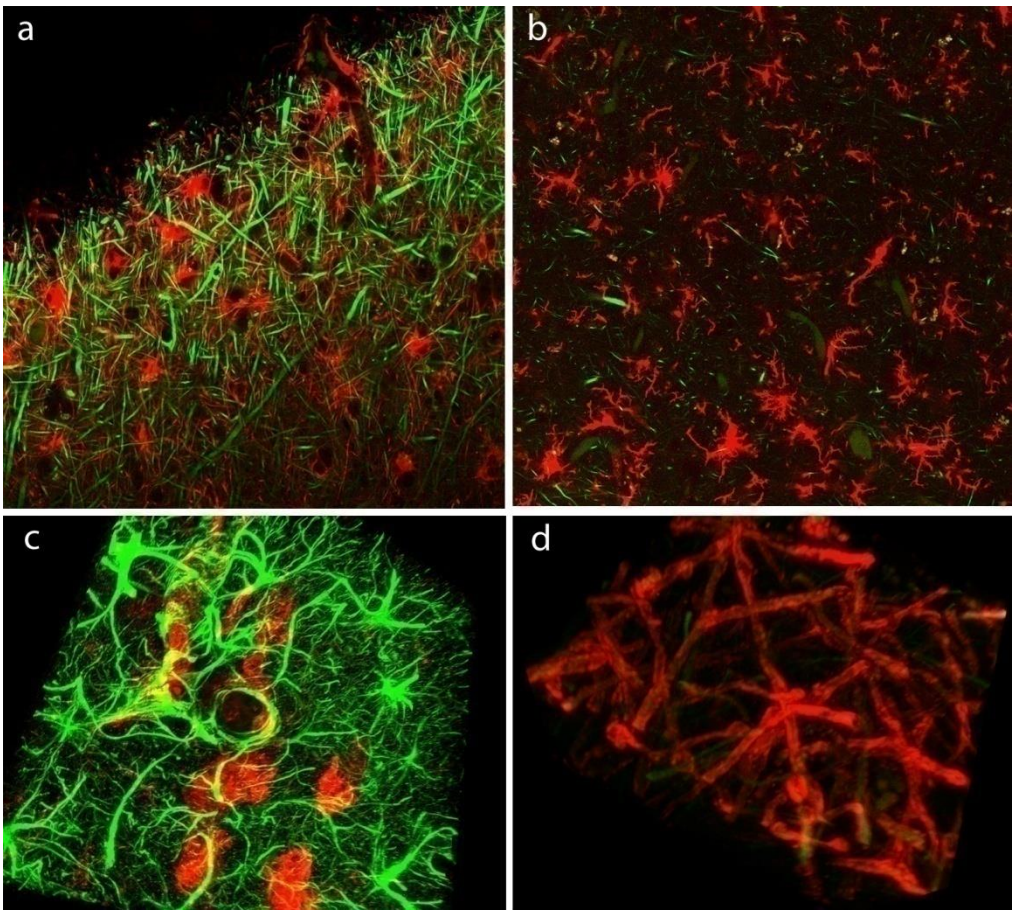

Figure 25 *Testing of different antibodies on 1mm thick, CLARITY processed experimental autoimmune encephalomyelitis (EAE) rat sections. (**a**) Astrocytes (GFAP_Cy3) and Axons (SMI-31_DL488). (**b**) Activated microglia (Iba-1_Cy3) and Axons (SMI-31_DL488). (**c**) 3D reconstruction of natural killer (NK) cells (GrB_Cy3) entering the brain parenchyma through the blood brain barrier (BBB) (GFAP_DL488) (blood vessel in the middle of the picture) (**d**) 3D reconstruction of myelin sheet (PLP_Cy3) wrapping around axons (SMI-31_DL488).*

The IHC protocol worked with every tested antibody and confocal microscopy was used for imaging. Uniform staining in x,y-direction (Figure 25 a,b) and up to the first 100µm in z-direction could be observed (Figure 25 c,d).

5.3 Staining in microwave

Cell culture dishes were incubated according to the staining procedure in microwave. In comparison with standard IHC protocols it was possible to achieve faster molecular labeling in cell culture (Figure 26).

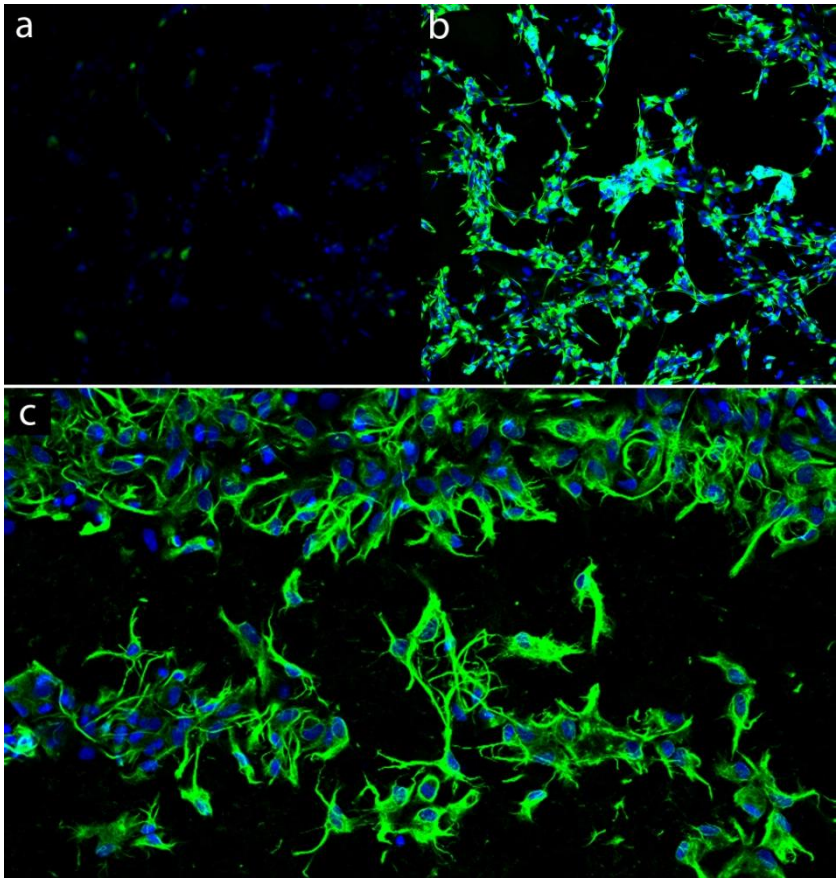

Figure 26 *Comparison of standard immunohistochemical (IHC) incubation with the microwave approach in astrocyte cell culture. The nuclear cores were labeled with DAPI (blue) the astrocytes were labeled with GFAP (green) (**a**) Normal IHC staining for 12 minutes with primary and 12 minutes with secondary antibody. Very week signal due to insufficient antibody binding time (**b**) Normal IHC staining for 60 minutes with primary and 60 minutes with secondary antibody. Good signal due to the sufficient binding time. (**c**) IHC staining in microwave for 12 minutes with primary and 12 minutes with secondary antibody. Very good signal due to enhanced antibody binding speed.*

5.4 iDISCO staining approach

Before starting with the staining protocol for iDISCO, the generated GFAP-F(ab')2-AF555 parts have been tested with a standard IHC protocol for their binding affinity to astrocytes in cell culture (Figure27).

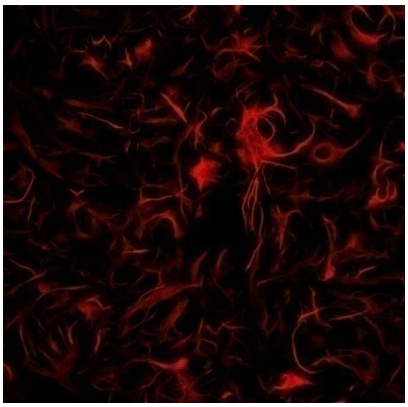

Figure 27 *Astrocyte cell culture stained with GFAP-F(ab')2-AF555.*

Thy1-GFP-M mouse hemispheres were processed according to the iDISCO protocol with different pretreatment approaches. These pretreatment approaches should facilitate better antibody penetration by removing the lipid membranes.

The methanol tissue pretreatment was used for one hemisphere of each brain, as a standard; and was compared to the other pretreatment approaches utilized for the another hemisphere (Figure 28). All the samples were incubated under same conditions on a shaking table with GFAP-F(ab')2-AF555 for 9 days at 37°C.

The supernatant was tested in astrocyte cell culture for remaining antibodies and showed in comparison to Figure 27 less but still detectable binding (Data not shown). The hemispheres displayed superficial labeling with every pretreatment approach, and in some cases patchy labeling of a bit deeper structures (Figure 28 a, b right hemisphere). In addition, the increased autofluorescence could be detected in the detergent-based pretreatment (Figure 28 b right hemisphere). All hemispheres displayed lower transparency in comparison to the 3-DISCO approach, resulting the blurry images (Figure 28). The tetrahydrofuran (THF) pretreatment has shown the least artifacts and best quantity of labeling.

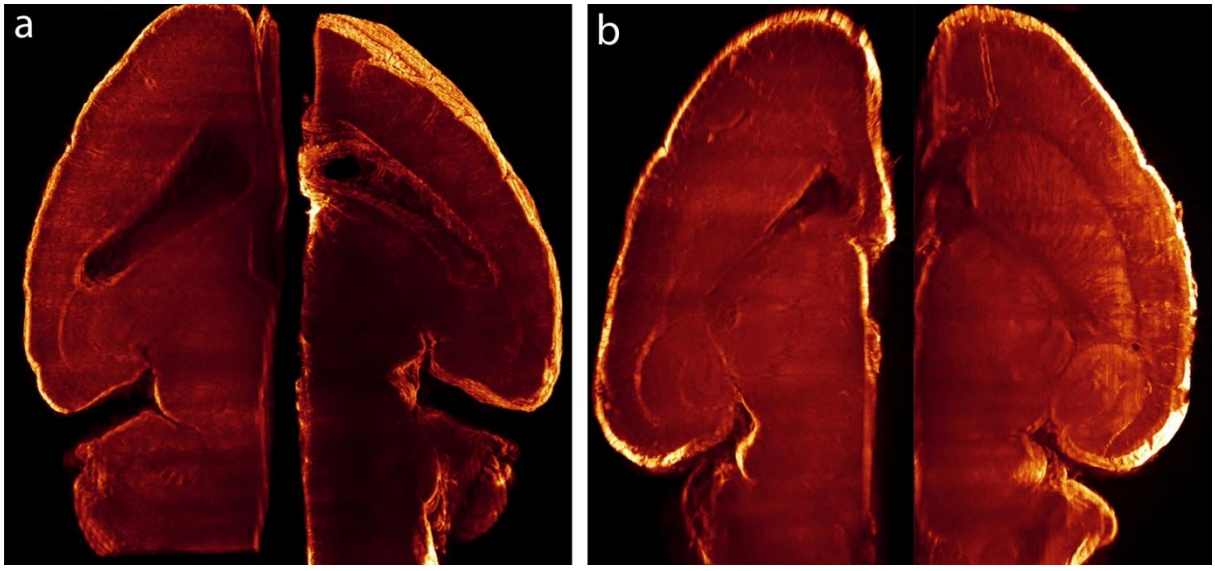

Figure 28 *Different iDISCO pretreatment approaches, labeled with GFAP-F(ab')2-AF555 parts. Left hemisphere in (a) and (b) was processed with methanol pretreatment approach. (**a**) The right hemisphere was processed according to the tetrahydrofuran (THF) approach, showing better transparency and labeling of structures than the left hemisphere.(**b**) The right hemisphere was processed according to the detergent pretreatment approach.*

5.5 Advanced light sheet microscopy

CLARITY cleared hemispheres were incubated in BrainClear and placed in a cuvette (Figure 18 at upper left corner). Optical sectioning was performed with a standard ultramicroscope (Figure 18) and one with aspheric lens system (Figure 19).

The aspheric system create a thinner and more homogeneous light sheet, resulting in better z-resolution and a sharper xy-resolution for larger specimen surface (Figure 29).

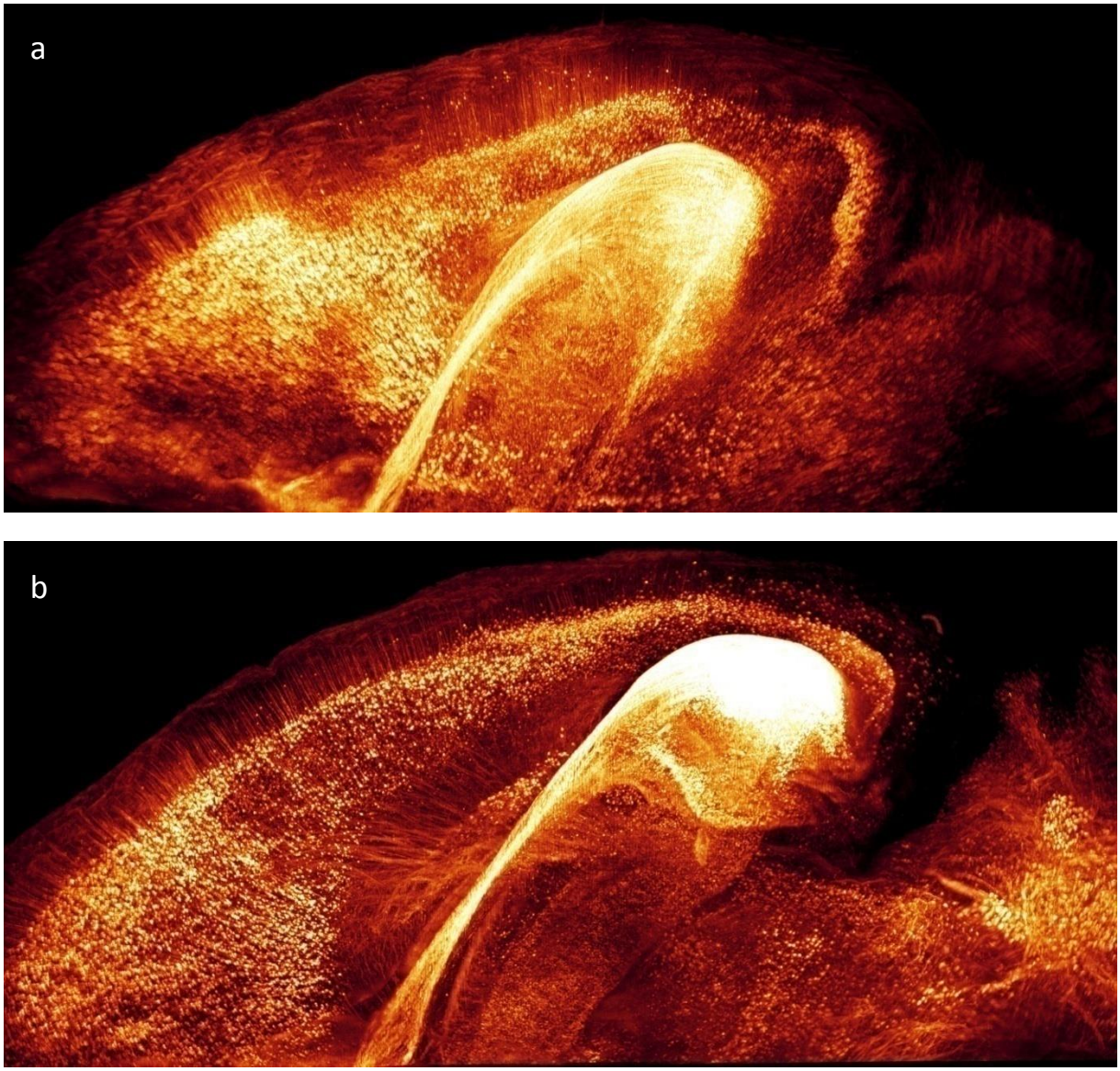

Figure 29 *Ultramircoscopy pictures (**a**) Image taken with a standard ultramicroscope, showing blurry areas at the borders of the samples, 2x objective N.A. 0.14 (0.63 post demagnification). (**b**) Image taken with a aspheric lens ultramicroscope system, showing overall sharpness, 2x objective N.A. 0.14 (0.5 post demagnification). Pictures kindle provided by Saiedeh Saghafi.*

6. Discussion

6.1 Tissue clearing

Initial attempts to establish the CLARITY method led to unsatisfactory results. Major problems are: the insufficient lipid removal, resulting in an opaque sample after RI matching, black depositions from precipitated buffer components on the tissue; massive, or in a worst case, complete loss of the fluorescent signal, sample destruction, due to the heat generation of the electric field and insufficient heat dissipation due to the low flow rate.

In order to minimize the tissue damage and to achieve the sufficient lipid removal, a new design of the efficient and stable electrophoretic tissue clearing-(ETC)-chamber, including the continuous flow of the SDS/boric acid buffer, temperature control (at 37°C), and low voltage application (15-20V) was indispensable (Figures 15 and 22a).

With the time, black sediment accumulates on the cathode. To avoid the transfer of the particles of that sediment into the specimen, the electrodes have been cleaned by reversing the polarity of the electric field. The electrode-cleaning was done after every processed sample, using a NaCl or KCL solution. The system should run for three minutes at a high voltage. Longer application of a strong electric field would result the accumulation of the sediment particles on the former anode.

The lower limit of the pH 7.5 of lipid-washing buffer, suggested in Chung et al., 2013 resulted in strong loss of fluorescent signal in our Thy1-GFP-M mouse model in comparison to a sample where the pH hasn't decrease below 8 (Figure 22). Our transgenic mouse model has a much weaker GFP expression than the model used in the original publication. By setting this new pH limit, fluorescence could be preserved better. This enables us to use the mouse model with a weak transgenic signal expression, reducing the risk of important information loss (Figure 21).

Further, refraction index (RI) matching solutions like 80% Glycerol, FocusClear or Histodenz provide the sufficient tissue transparency for a short period of time. Within the longer incubation time, the sample turns opaque and its fluorescent signal gets quenched. It is

suggested to store the samples in PBS after imaging (Tomer et al., 2014). The high price of some of these RI-matching solutions, i.e. FocusClear, and the storage of the samples in a different medium makes the process expensive and the handling of the samples very unpractical.

So far there is no publication mentioning the RI medium that preserves the fluorescence and enables long-term storage. Comparing to the commercially available RI-matching substances, with BrainClear we achieved superior results showing very good tissue transparency and transgenic signal preservation, thereby enabling storage in the RI medium (Figure 23, 24).

6.2 Tissue staining

Passive antibody staining in a thick tissue is a very long incubation process resulting in uneven binding, with over-labeling in the outer regions and decrease of labeling within the deeper tissue (Figure 30).

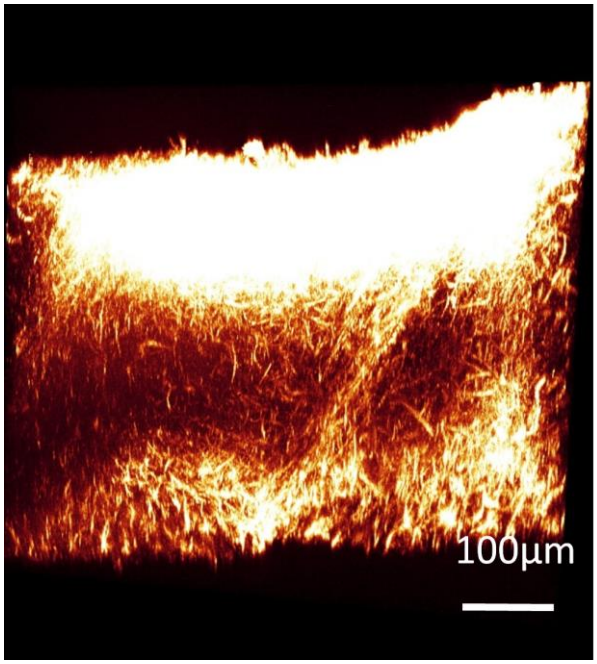

Figure 30 *Antibody binding gradient of astrocytes labeled with GFAP-F(ab')2-AF555. Picture shows over labeling on the surface and week labeling in the middle of the tissue.*

The antibodies bind faster to the available epitops then they migrate inside the tissue. One attempt to shorten that process is the use of antibodies that have a directly conjugated fluorophore, thereby avoiding the incubation step with the fluorophore coupled secondary antibody. Regarding the processing time, this shortens the procedure by half. However, this doesn't change the binding gradient and uneven labeling at the end.

In order to enhance the tissue penetration we tried to use the smaller labeling molecules (Holliger and Hudson, 2005). The idea behind is to minimize the size-dependent resistance of the molecules which need to enter the sample. The smallest of the developed molecules are the nanobodies or single domains with a size of 15kDa compared to an IgG with 150kDa. However, the range of these molecules is very limited and they display a very weak signal.

The F(ab')2 parts used in our experiments have a size of 110kDa, a fluorophore coupled one with a high ε and high specificity due to the removal of the unspecific binding (Fc) domain. Nevertheless, a binding gradient still occurs (Figure 30).

Another approach to facilitate the access of deeper tissue penetration for labeling molecules is to change the consistency of the specimen. By decreasing the acrylamide component, it's been aimed to enlarge the pore- size of the hydrogel embedded samples. That led to an unstable polymer meshwork and has shown no major improvement of the antibody penetration (Li et al., 2015). Dehydration and rehydration of the tissue or chemically harsh pretreatment, with the highly concentrated detergents, show good data with the small samples (Renier et al., 2014; Susaki et al., 2014) but remain short on convincing results for the bigger specimens, i.e. mouse hemisphere or whole brain. The performed IHC incubation with CLARITY processed rat brain-sections and the iDISCO approach shown above (Figure 25, 28, 30) displayed just superficial tissue labeling and the gradient binding of the antibodies. Taken together all of these facts indicate, that passive incubation is insufficient for larger samples.

Active antibody penetration has been performed by the periodically heating and thawing of samples or by the microwave approach (above). It was possible to perform fast labeling of cell culture with commercially available microwave (Figure 25) but the processing of larger specimens turned out to be very challenging. Maintaining the constant temperature, during longer incubation steps by cooling tissue-containing chamber with dry ice was very difficult.

The temperature distribution in the microwaves is not uniform. Further, the dry ice is not affected by the microwaves but still evaporation occurs. This leads to a scope of more than 25°C difference between the incubation steps and making an estimation of the duration of multiple cooling periods demanding. Additionally, complete loss of signal in whole Thy1-GFP-M mouse brain could be observed (data not shown).

The uneven temperature distribution and the complete quenching of transgenic signal limit the application of this approach. However, professional temperature controlled microwaves exist, i.e. PELCO BioWave® Pro, but they are very expensive and so far no publication mentioned this approach in combination with large tissue samples.

6.3 Imaging with ultramicroscopy

Whole-brain imaging with single-cell resolution is one of the most important challenges in neuroscience, as it is required for the complex-system identification and analysis of cellular networks in the brain. Scanning microscopes, i.e. confocal or 2-photon, in combination with various cross-sectional tomography methods can generate high-resolution images throughout the brain. However, the slow speed of scanning, along with the large data storage capacities required, and the expensive specialized equipment make this approach impractical for the large samples.
Light sheet fluorescence microscopy (LSFM) has recently emerged as a good alternative for imaging the large, optically clear specimens. The advantages of LSFM over the point-scanning methods are a high acquisition speed, reduced sample bleaching, large field of view and a high dynamic range.

In comparison with other LSFM designs, the aspheric lens ultramicroscope system has the highest Rayleigh range in conjunction with the smallest beam diameter (2µm) along the line of uniform intensity (Saghafi et al., 2014). The thin light sheet enables image acquisition with high z-axis resolution, which is a prerequisite for further 3D reconstruction of large specimens.

We recorded CLARITY-cleared mouse brain hemispheres with the standard ultramicroscopy and with aspheric lens ultramicroscope. The 3D reconstructed images of GFP-expressing mouse hemispheres have demonstrated a higher quality of optical sectioning with the aspheric lens system (Figure 29).

Still, LSFM approaches are developing fast and probably, a 3D-superresolution imaging with stimulated emission depletion (STED) light sheets will be available in near future.

In addition, the easy handling and the fast developing methods of tissue clearing will make LSFM more accessible to other scientists and broaden the field of application.

7.Conclusion

We demonstrated an improved protocol for CLARITY showing better transparency, more preserved fluorescent signal and the possibility of long term storage in the RI medium. In combination with the aspheric lens ultramicroscopy system high resolution data of whole mouse brains could be obtained.

Immunolabeling remained a big obstacle and the goal to stain a whole mouse brain could not be reached.

The use of commercial microwave increased the binding speed of the antibodies in cell culture. However, the loss of fluorescence, the difficulty in maintaining a specific temperature and the unpractical handling turned it out to be not applicable for thick samples.

However, we tried different methods to stain large specimens and succeeded to label thick tissue sample. Nevertheless, further optimization of the protocols is required.

8. Acknowledgments

First of all I would like to thank Prof. Dr. Dodt for giving me the opportunity to work in his lab on my master-thesis. He was very patient with me and he was there when I needed help, and I am very thankful for that.

Especially I want to thank Dr. Christian Hahn, Dr. Klaus Becker, Inna Sabdyusheva Litschauer, Dipl.-Phys. and Dr. Saiedeh Saghafi. I am very grateful and lucky to have helping colleagues with whom I can work but also laugh a lot. They provided valuable information on my topic and shared their knowledge whenever needed.

Furthermore I want to thank my colleagues: Martina Wanis, Dr. Simon Hametner, Joana Santos, Dr. Nina Jähring, Bella Bauer, Ruben Russel Schulz, Tobias Zrzavy and Dr. Lukas Haider for very interesting and inspiring talks and new ideas.

My special gratitude belongs to Bleranda Zeka, Bahar Camurdanoglu and Florain Kellner who have also supported me during practical work and thereby saved me a lot of time in the laboratory.
Most of all I want to thank my parents Tomislav and Marina, my sister Nika, my girlfriend Laura and the rest of my family and friends, who have always supported me and helped me to manage my degree.

9. References

Alnuami, A.A., Zeedi, B., Qadri, S.M., and Ashraf, S.S. (2008). Oxyradical-induced GFP damage and loss of fluorescence. Int J Biol Macromol *43*, 182-186.

Becker, K., Jahrling, N., Saghafi, S., Weiler, R., and Dodt, H.U. (2012). Chemical clearing and dehydration of GFP expressing mouse brains. PLoS One *7*, e33916.

Bouchard, M.B., Voleti, V., Mendes, C.S., Lacefield, C., Grueber, W.B., Mann, R.S., Bruno, R.M., and Hillman, E.M. (2015). Swept confocally-aligned planar excitation (SCAPE) microscopy for high speed volumetric imaging of behaving organisms. Nat Photonics *9*, 113-119.

Bunka, D.H., and Stockley, P.G. (2006). Aptamers come of age–at last. Nature Reviews Microbiology *4*, 588-596.

Chen, B.C., Legant, W.R., Wang, K., Shao, L., Milkie, D.E., Davidson, M.W., Janetopoulos, C., Wu, X.S., Hammer, J.A., 3rd, Liu, Z.*, et al.* (2014). Lattice light-sheet microscopy: imaging molecules to embryos at high spatiotemporal resolution. Science *346*, 1257998.

Chen, F., Tillberg, P.W., and Boyden, E.S. (2015). Optical imaging. Expansion microscopy. Science *347*, 543-548.

Chiang, A.S., Lin, W.Y., Liu, H.P., Pszczolkowski, M.A., Fu, T.F., Chiu, S.L., and Holbrook, G.L. (2002). Insect NMDA receptors mediate juvenile hormone biosynthesis. Proc Natl Acad Sci U S A *99*, 37-42.

Chung, K., Wallace, J., Kim, S.Y., Kalyanasundaram, S., Andalman, A.S., Davidson, T.J., Mirzabekov, J.J., Zalocusky, K.A., Mattis, J., Denisin, A.K.*, et al.* (2013). Structural and molecular interrogation of intact biological systems. Nature *497*, 332-337.

Costantini, I., Ghobril, J.P., Di Giovanna, A.P., Allegra Mascaro, A.L., Silvestri, L., Mullenbroich, M.C., Onofri, L., Conti, V., Vanzi, F., Sacconi, L.*, et al.* (2015). A versatile clearing agent for multi-modal brain imaging. Sci Rep *5*, 9808.

Denk, W., and Horstmann, H. (2004). Serial block-face scanning electron microscopy to reconstruct three-dimensional tissue nanostructure. PLoS Biol *2*, e329.

Dodt, H.U., Leischner, U., Schierloh, A., Jahrling, N., Mauch, C.P., Deininger, K., Deussing, J.M., Eder, M., Zieglgansberger, W., and Becker, K. (2007). Ultramicroscopy: three-dimensional visualization of neuronal networks in the whole mouse brain. Nat Methods *4*, 331-336.

Erturk, A., Mauch, C.P., Hellal, F., Forstner, F., Keck, T., Becker, K., Jahrling, N., Steffens, H., Richter, M., Hubener, M.*, et al.* (2012). Three-dimensional imaging of the unsectioned adult spinal cord to assess axon regeneration and glial responses after injury. Nat Med *18*, 166-171.

Feng, G., Mellor, R.H., Bernstein, M., Keller-Peck, C., Nguyen, Q.T., Wallace, M., Nerbonne, J.M., Lichtman, J.W., and Sanes, J.R. (2000). Imaging neuronal subsets in transgenic mice expressing multiple spectral variants of GFP. Neuron *28*, 41-51.

Ferris, A.M., Giberson, R.T., Sanders, M.A., and Day, J.R. (2009). Advanced laboratory techniques for sample processing and immunolabeling using microwave radiation. J Neurosci Methods *182*, 157-164.

Gong, H., Zeng, S., Yan, C., Lv, X., Yang, Z., Xu, T., Feng, Z., Ding, W., Qi, X., Li, A.*, et al.* (2013). Continuously tracing brain-wide long-distance axonal projections in mice at a one-micron voxel resolution. Neuroimage *74*, 87-98.

Hama, H., Kurokawa, H., Kawano, H., Ando, R., Shimogori, T., Noda, H., Fukami, K., Sakaue-Sawano, A., and Miyawaki, A. (2011). Scale: a chemical approach for fluorescence imaging and reconstruction of transparent mouse brain. Nat Neurosci *14*, 1481-1488.

Helmchen, F., and Denk, W. (2005). Deep tissue two-photon microscopy. Nat Methods *2*, 932-940.

Holekamp, T.F., Turaga, D., and Holy, T.E. (2008). Fast three-dimensional fluorescence imaging of activity in neural populations by objective-coupled planar illumination microscopy. Neuron *57*, 661-672.

Holliger, P., and Hudson, P.J. (2005). Engineered antibody fragments and the rise of single domains. Nature biotechnology *23*, 1126-1136.

Hou, B., Zhang, D., Zhao, S., Wei, M., Yang, Z., Wang, S., Wang, J., Zhang, X., Liu, B., Fan, L*., et al.* (2015). Scalable and DiI-compatible optical clearance of the mammalian brain. Front Neuroanat *9*, 19.

Huisken, J., Swoger, J., Del Bene, F., Wittbrodt, J., and Stelzer, E.H. (2004). Optical sectioning deep inside live embryos by selective plane illumination microscopy. Science *305*, 1007-1009.

Ichimura, K., Miyazaki, N., Sadayama, S., Murata, K., Koike, M., Nakamura, K., Ohta, K., and Sakai, T. (2015). Three-dimensional architecture of podocytes revealed by block-face scanning electron microscopy. Sci Rep *5*, 8993.

Johnson, G.A., Cofer, G.P., Gewalt, S.L., and Hedlund, L.W. (2002). Morphologic phenotyping with MR microscopy: the visible mouse. Radiology *222*, 789-793.

Kalender, W.A. (2005). CT: the unexpected evolution of an imaging modality. Eur Radiol *15 Suppl 4*, D21-24.

Ke, M.T., Fujimoto, S., and Imai, T. (2013). SeeDB: a simple and morphology-preserving optical clearing agent for neuronal circuit reconstruction. Nat Neurosci *16*, 1154-1161.

Kuwajima, T., Sitko, A.A., Bhansali, P., Jurgens, C., Guido, W., and Mason, C. (2013). ClearT: a detergent- and solvent-free clearing method for neuronal and non-neuronal tissue. Development *140*, 1364-1368.

Li, A., Gong, H., Zhang, B., Wang, Q., Yan, C., Wu, J., Liu, Q., Zeng, S., and Luo, Q. (2010). Micro-optical sectioning tomography to obtain a high-resolution atlas of the mouse brain. Science *330*, 1404-1408.

Li, J., Czajkowsky, D.M., Li, X., and Shao, Z. (2015). Fast immuno-labeling by electrophoretically driven infiltration for intact tissue imaging. Sci Rep *5*, 10640.

Linington, C., Berger, T., Perry, L., Weerth, S., Hinze-Selch, D., Zhang, Y., Lu, H.C., Lassmann, H., and Wekerle, H. (1993). T cells specific for the myelin oligodendrocyte glycoprotein mediate an unusual autoimmune inflammatory response in the central nervous system. Eur J Immunol *23*, 1364-1372.

Linington, C., Bradl, M., Lassmann, H., Brunner, C., and Vass, K. (1988). Augmentation of demyelination in rat acute allergic encephalomyelitis by circulating mouse monoclonal antibodies directed against a myelin/oligodendrocyte glycoprotein. Am J Pathol *130*, 443-454.

Mayerich, D., Abbott, L., and McCormick, B. (2008). Knife-edge scanning microscopy for imaging and reconstruction of three-dimensional anatomical structures of the mouse brain. J Microsc *231*, 134-143.

Meglinski, I., Churmakov, D., Bashkatov, A., Genina, E., and Tuchin, V. (2004). The enhancement of confocal images of tissues at bulk optical immersion. arXiv preprint physics/0401104.

Micheva, K.D., and Smith, S.J. (2007). Array tomography: a new tool for imaging the molecular architecture and ultrastructure of neural circuits. Neuron *55*, 25-36.

Mokhtarian, F., McFarlin, D.E., and Raine, C.S. (1984). Adoptive transfer of myelin basic protein-sensitized T cells produces chronic relapsing demyelinating disease in mice. Nature *309*, 356-358.

Morris-Downes, M.M., Smith, P.A., Rundle, J.L., Piddlesden, S.J., Baker, D., Pham-Dinh, D., Heijmans, N., and Amor, S. (2002). Pathological and regulatory effects of anti-myelin antibodies in experimental allergic encephalomyelitis in mice. J Neuroimmunol *125*, 114-124.

Munoz, T.E., Giberson, R.T., Demaree, R., and Day, J.R. (2004). Microwave-assisted immunostaining: a new approach yields fast and consistent results. J Neurosci Methods *137*, 133-139.

Oh, S.W., Harris, J.A., Ng, L., Winslow, B., Cain, N., Mihalas, S., Wang, Q., Lau, C., Kuan, L., Henry, A.M*., et al.* (2014). A mesoscale connectome of the mouse brain. Nature *508*, 207-214.

Owens, K., Park, J.H., and Kristian, T. (2013). Utilizing commercial microwave for rapid and effective immunostaining. J Neurosci Methods *219*, 20-26.

Planchon, T.A., Gao, L., Milkie, D.E., Davidson, M.W., Galbraith, J.A., Galbraith, C.G., and Betzig, E. (2011). Rapid three-dimensional isotropic imaging of living cells using Bessel beam plane illumination. Nat Methods *8*, 417-423.

Ragan, T., Kadiri, L.R., Venkataraju, K.U., Bahlmann, K., Sutin, J., Taranda, J., Arganda-Carreras, I., Kim, Y., Seung, H.S., and Osten, P. (2012). Serial two-photon tomography for automated ex vivo mouse brain imaging. Nat Methods *9*, 255-258.

Ragan, T., Sylvan, J.D., Kim, K.H., Huang, H., Bahlmann, K., Lee, R.T., and So, P.T. (2007). High-resolution whole organ imaging using two-photon tissue cytometry. J Biomed Opt *12*, 014015.

Renier, N., Wu, Z., Simon, D.J., Yang, J., Ariel, P., and Tessier-Lavigne, M. (2014). iDISCO: a simple, rapid method to immunolabel large tissue samples for volume imaging. Cell *159*, 896-910.

Richardson, D.S., and Lichtman, J.W. (2015). Clarifying Tissue Clearing. Cell *162*, 246-257.

Saghafi, S., Becker, K., Hahn, C., and Dodt, H.U. (2014). 3D-ultramicroscopy utilizing aspheric optics. J Biophotonics *7*, 117-125.

Sharpe, J., Ahlgren, U., Perry, P., Hill, B., Ross, A., Hecksher-Sorensen, J., Baldock, R., and Davidson, D. (2002). Optical projection tomography as a tool for 3D microscopy and gene expression studies. Science *296*, 541-545.

Siedentopf, H., and Zsigmondy, R. (1902). Uber Sichtbarmachung und Größenbestimmung ultramikoskopischer Teilchen, mit besonderer Anwendung auf Goldrubingläser. Annalen der Physik *315*, 1-39.

Spalteholz, W. (1914). Über das Durchsichtigmachen von menschlichen und tierischen Präparaten. Hierzel, Leipzig *2*, 91.

Staudt, T., Lang, M.C., Medda, R., Engelhardt, J., and Hell, S.W. (2007). 2,2'-thiodiethanol: a new water soluble mounting medium for high resolution optical microscopy. Microsc Res Tech *70*, 1-9.

Steinke, H., and Wolff, W. (2001). A modified Spalteholz technique with preservation of the histology. Ann Anat *183*, 91-95.

Streicher, J., Donat, M.A., Strauss, B., Sporle, R., Schughart, K., and Muller, G.B. (2000). Computer-based three-dimensional visualization of developmental gene expression. Nat Genet *25*, 147-152.

Susaki, E.A., Tainaka, K., Perrin, D., Kishino, F., Tawara, T., Watanabe, T.M., Yokoyama, C., Onoe, H., Eguchi, M., Yamaguchi, S.*, et al.* (2014). Whole-brain imaging with single-cell resolution using chemical cocktails and computational analysis. Cell *157*, 726-739.

Tainaka, K., Kubota, S.I., Suyama, T.Q., Susaki, E.A., Perrin, D., Ukai-Tadenuma, M., Ukai, H., and Ueda, H.R. (2014). Whole-body imaging with single-cell resolution by tissue decolorization. Cell *159*, 911-924.

Temel, S.G., Minbay, F.Z., Kahveci, Z., and Jennes, L. (2006). Microwave-assisted antigen retrieval and incubation with cox-2 antibody of archival paraffin-embedded human oligodendroglioma and astrocytomas. J Neurosci Methods *156*, 154-160.

Toga, A.W., Goldkorn, A., Ambach, K., Chao, K., Quinn, B.C., and Yao, P. (1997). Postmortem cryosectioning as an anatomic reference for human brain mapping. Comput Med Imaging Graph *21*, 131-141.

Tomer, R., Ye, L., Hsueh, B., and Deisseroth, K. (2014). Advanced CLARITY for rapid and high-resolution imaging of intact tissues. Nat Protoc *9*, 1682-1697.

Tsai, P.S., Kaufhold, J.P., Blinder, P., Friedman, B., Drew, P.J., Karten, H.J., Lyden, P.D., and Kleinfeld, D. (2009). Correlations of neuronal and microvascular densities in murine cortex revealed by direct counting and colocalization of nuclei and vessels. J Neurosci *29*, 14553-14570.

Tyszka, J.M., Fraser, S.E., and Jacobs, R.E. (2005). Magnetic resonance microscopy: recent advances and applications. Curr Opin Biotechnol *16*, 93-99.

Weninger, W.J., and Mohun, T. (2002). Phenotyping transgenic embryos: a rapid 3-D screening method based on episcopic fluorescence image capturing. Nat Genet *30*, 59-65.

Wu, Y., Wawrzusin, P., Senseney, J., Fischer, R.S., Christensen, R., Santella, A., York, A.G., Winter, P.W., Waterman, C.M., Bao, Z.*, et al.* (2013). Spatially isotropic four-dimensional imaging with dual-view plane illumination microscopy. Nat Biotechnol *31*, 1032-1038.

Xiong, H., Zhou, Z., Zhu, M., Lv, X., Li, A., Li, S., Li, L., Yang, T., Wang, S., Yang, Z.*, et al.* (2014). Chemical reactivation of quenched fluorescent protein molecules enables resin-embedded fluorescence microimaging. Nat Commun *5*, 3992.

Yang, B., Treweek, J.B., Kulkarni, R.P., Deverman, B.E., Chen, C.K., Lubeck, E., Shah, S., Cai, L., and Gradinaru, V. (2014). Single-cell phenotyping within transparent intact tissue through whole-body clearing. Cell *158*, 945-958.

Zheng, T., Yang, Z., Li, A., Lv, X., Zhou, Z., Wang, X., Qi, X., Li, S., Luo, Q., Gong, H.*, et al.* (2013). Visualization of brain circuits using two-photon fluorescence micro-optical sectioning tomography. Opt Express *21*, 9839-9850.

Curriculum vitae

Deutsch:

Ausbildung

September 2015	Universitäts Assistent auf der TU Wien und Start des PhD Studiums in "Biomedical Engineering" auf der TU Wien, Österreich
Juni 2014	Master Abschluss mit Auszeichnung in Molecularer Biology mit Hauptaugenmerk auf "Neuroscience"
2011-2014	Master in Molekularer Biologie (mit Hauptaugenmerk auf "Neuroscience") und Master in Immunologie und Mikrobiologie (mit Hauptaugenmerk auf Immunologie)
2013-2015	Praktische Arbeit für die zweite Masterarbeit auf dem CBR (Center for Brain Research) in dem Department für Bioelektronik Uni Wien, Österreich
2012-2014	Praktische Arbeit für die Masterarbeit auf dem CBR (Center for Brain Research) in der Abteilung für Neuroimmunologie Uni Wien, Österreich
2007-2011	Bachelor in Genetik und Mikrobiologie auf dem MFPL (Max F. Perutz Laboratories) Uni Wien, Österreich
2007	Militärdienst in der **"**4ten. Gardekompanie", Österreich
1998-2006	"Bundesgymnasium und Bundesrealgymnasium Zirkusgasse", Österreich

Weitere Ausbildung und Praktika

Juni 2014 Teilgenommen bei der **"**9th FENS Forum of Neuroscience" - Mailand

July 2012 PADI (Professional Association of Diving Instructors) "Divemaster" Ausbildung

Aug.-Sep. 2011 Zwei Monatiges Praktikum bei Baxter Innovations GmbH, Orth an der Donau, Österreich. Thema: "Cellular Processing" bei "Good Laboratory Practice" (GLP) Bedingungen in einem Sicherheitsstufe drei Labor

Jan. 2011 Bioinformatik Kurs, auf dem IMP (Institute of Molecular Pathology)

Sep. 2010 Zwei Monatiges Praktikum bei Baxter Innovations GmbH, Orth an der Donau, Österreich. Thema: "Cellular Processing" bei "Good Laboratory Practice" (GLP) Bedingungen in einem Sicherheitsstufe drei Labor

Oct. 2010 Praktischer Kurs: "Molecular analysis of gene expression", auf der Krebsforschung, Meduni Wien

Mar. 2010 Praktischer Kurs: Bioverfahrenstechnick, auf der TU Wien (Technical University)

Vorträge

1st CLARITY USERS Meeting, 7th April 2014
London, United Kingdom. Immunohistochemistry and 3D reconstruction of clarified tissue.

Poster Präsentationen

5th Neuroscience Vienna Network Meeting, will be on 26th May 2015
Vienna, Austria. Deep Tissue Imaging with Improved Optical Clearing

Publikationen

Hans-Ulrich Dodt, Saiedeh Saghafi[1], Klaus Becker, Nina Jährling, Christian Hahn, **Marko Pende**, Martina Wanis, Axel Niendorf "Ultramicroscopy: Development and Outlook", *SPIE*

Maria Pohl, Bleranda Zeka, Andreas Horner, Christine Siligan, Kathrin Schanda, **Marko Pende**, Corinna Knopf, Martin Vietauer, Andreas Pohlmann, Markus Reindl, Leopold Schmetterer, Hans Lassmann and Monika Bradl "The eye as target of aquaporin-specific T cells and NMO-IgG", *in preparation*

English:

Education

September 2015	University assistant at the TU Wien and start of PhD in "Biomedical engineering" at the TU Wien, Austria
June 2014	Master degree with honor in Molecular Biology with main focus on Neuroscience
2011-2014	Master in Molecular Biology (with main focus on Neuroscience) and Master in Immunology and Microbiology (with main focus on Immunology)
2013-2015	Work for second masterthesis at the CBR (Center for Brain research) at the Department for Bioelectronics Uni Wien, Austria
2012-2014	Work for masterthesis at the CBR (Center for Brain research) at the department for Neuroimmunology Uni Wien, Austria.
2007-2011	Bachelor in Genetic and Microbiology at the MFPL (Max F. Perutz Laboratories) Uni Wien, Austria.
2007	Military service in the Austrian Armed Forces "4. Gardekompanie", Austria
1998-2006	Highschool "Bundesgymnasium und Bundesrealgymnasium Zirkusgasse", Austria

Further education and internships

June 2014 participated at the 9th FENS Forum of Neuroscience - Milan

July 2012 PADI (Professional Association of Diving Instructors) Divemaster certification

Aug.-Sep. 2011 Two months internship in Baxter Innovations GmbH, Orth an der Donau, Austria. Subject: Cellular Processing under Good Laboratory Practice (GLP) conditions in a stage three safety laboratory

Jan. 2011 Bioinformatics course, at the IMP (Institute of Molecular Pathology)

Sep. 2010 Internship in Baxter Innovations GmbH, Orth an der Donau, Austria. Subject: Cellular Processing under Good Laboratory Practice (GLP) conditions in a stage three safety laboratory

Oct. 2010 Practical course: Molecular analysis of gene expression, at the Cancer Research Institute, Medical University of Vienna.

Mar. 2010 Practical course: Bioverfahrenstechnick, at the TU Wien (Technical University)

Oral presentations

1st CLARITY USERS Meeting, 7th April 2014
London, United Kingdom. Immunohistochemistry and 3D reconstruction of clarified tissue.

Poster presentations

5th Neuroscience Vienna Network Meeting, will be on 26th May 2015
Vienna, Austria. Deep Tissue Imaging with Improved Optical Clearing

Publications

Hans-Ulrich Dodt, Saiedeh Saghafi[1], Klaus Becker, Nina Jährling, Christian Hahn, **Marko Pende**, Martina Wanis, Axel Niendorf "Ultramicroscopy: Development and Outlook", *SPIE*

Maria Pohl, Bleranda Zeka, Andreas Horner, Christine Siligan, Kathrin Schanda, **Marko Pende**, Corinna Knopf, Martin Vietauer, Andreas Pohlmann, Markus Reindl, Leopold Schmetterer, Hans Lassmann and Monika Bradl "The eye as target of aquaporin-specific T cells and NMO-IgG", *in preparation*